



Cite this: *J. Mater. Chem. A*, 2023, 11, 1013

Toward efficient hybrid solar cells comprising quantum dots and organic materials: progress, strategies, and perspectives

Junwei Liu,^{ab} Jingjing Wang,^{bc} Yang Liu,^b Kaihu Xian,^b Kangkang Zhou,^b Junjiang Wu,^b Sunsun Li,^d Wenchao Zhao,^{*a} Zhihua Zhou^{*a} and Long Ye^{bce}

The emerging solution-processing photovoltaic technologies, e.g., quantum dot (QD) and organic solar cells, have witnessed unprecedented progress in the past decade. Nevertheless, both technologies have their own merits, holding promising potential to be leveraged for mutual win. Herein, a comprehensive and critical review of the state-of-the-art hybrid solar cells with three promising QDs (lead chalcogenide QDs, AgBiS₂ QDs, and perovskite QDs) is delivered with the goal of further enhancing their performance and stability for large-scale applications. Firstly, we discussed the working principles of hybrid solar cells and highlighted the combined support of various structures. Subsequently, QD passivation with organic ligands was further outlined, focusing on further enhancing the performance of QD solar cells. Then, there is an in-depth discussion on worldwide research efforts to enhance the performance and stability of hybrid devices, including bulk-heterojunction, bilayer, and tandem structures. Finally, the remaining open challenges and our insights are presented to offer promising research directions for further performance breakthrough.

Received 30th September 2022
Accepted 23rd November 2022

DOI: 10.1039/d2ta07671c

rsc.li/materials-a

1. Introduction

With the ever-increasing demand for energy and escalating environmental issues stemming from fossil fuel combustion,

the pursuit for sustainable and clean energy harvesting technologies has been at the center of the ongoing research efforts in the 21st century. Solar energy harvesting, one of the promising clean technologies, has attracted worldwide and consistent interest owing to its great potential to offset global energy

^aCo-Innovation Center of Efficient Processing and Utilization of Forest Resources, College of Materials Science and Engineering, Nanjing Forestry University, Nanjing 210037, China. E-mail: wenchaozhao@njfu.edu.cn

^bSchool of Environmental Science and Engineering, School of Materials Science and Engineering, Tianjin Key Laboratory of Molecular Optoelectronic Sciences, Tianjin University, Collaborative Innovation Center of Chemical Science and Engineering (Tianjin), Tianjin, 300350, China. E-mail: zhuazhou@tju.edu.cn; yelong@tju.edu.cn

^cState Key Laboratory of Applied Optics, Changchun Institute of Optics, Fine Mechanics and Physics, Chinese Academy of Sciences, Changchun, China

^dKey Laboratory of Flexible Electronics (KLOFE) and Institute of Advanced Materials (IAM), Nanjing Tech University (NanjingTech), Nanjing 211816, China

^eHubei Longzhong Laboratory, Xiangyang 441000, China



Junwei Liu is currently a joint PhD student in the groups of Prof. Zhihua Zhou and Prof. Long Ye at Tianjin University. He received his bachelor's and master's degrees from the School of Environmental Science and Engineering of Tianjin University in 2016 and 2019, respectively. His research is focused on radiative cooling and low-cost organic/hybrid solar cells.



Jingjing Wang is currently a graduate student at the School of Materials Science & Engineering, Tianjin University under the direction of Prof. Long Ye. She earned her bachelors degree in Polymer Materials & Engineering from Zhengzhou University in July 2021. Her research focuses on the performance optimization of low-cost organic/quantum dot solar cells.

consumption in view of the ever-growing global demand. Photovoltaics or solar cells, which directly convert solar energy into electricity, hold great promise for energy conversion in a sustainable and economical way.^{1–5} Crucially, the share of worldwide photovoltaics in clean energy production is expected to grow from 6.6% in 2017 to 21.8% in 2030, which certainly requires increasing research efforts to fulfill this target.⁶ Current commercialized photovoltaic modules still greatly rely on indirect bandgap crystalline silicon, which has nearly approached the theoretical maximum efficiency, albeit some notable application limitations in lightweight and flexible electronics and beyond.^{7–9}

Accordingly, some of these emerging solution-processing photovoltaics, *e.g.*, organic solar cells (OSCs)^{10–14} and quantum dot solar cells (QDSCs),^{15–19} have witnessed unprecedented progress in solar energy harvesting. Nevertheless, both technologies have their own merits, offering mutual benefits when combined each other. For instance, organic photovoltaic materials generally exhibit the strong absorption, great structure tunability, light weight, and high flexibility^{20–24} compared to their counterparts, *e.g.*, perovskite materials (Fig. 1a). Moreover, OSCs deliver striking efficiencies close to those of the silicon counterparts.^{25–29} Nevertheless, most top-notch OSCs can seldom harvest the infrared light beyond 1000 nm, which has placed great restrictions on their further performance enhancement.^{30–32} In addition, the strong exciton binding energy of most organic photovoltaic materials has impeded exciton dissociation, which has aroused a great demand for bulk heterojunction to obtain high OSC performance. The unsatisfactory phase stability and the notorious air and illumination degradation issues also place great restrictions on their applications.^{33–36} Furthermore, high-performance OSC systems, such as PM6:Y6 blend, generally endure high material cost and harsh processing, which further block the commercialization of OSCs (Fig. 1a, 2a and b).^{37,38}

Instead, lead chalcogenide QDSCs have proved to be promising candidates for high-stability and low-cost photovoltaics.^{39–41} For instance, lead chalcogenide QDSCs can retain ~80% of their initial efficiency after 1000 h of continuous illumination and over 90% of their initial performance after one year of ambient storage.^{42,43} Concomitantly, lead chalcogenide

QD inks present the strikingly low cost of ~6 \$ per g, which will greatly reduce the deployment expenses of QD photovoltaic modules.^{44–46} In addition, lead chalcogenide QDs generally exhibit broad bandgap tunability and absorption stemming from quantum confinement, which endows a broad absorption range even up to ~2000 nm.^{47–49} Except for quantum confinement, surface ligands, which are essential for QD stability, hold a great impact on QD electrical properties. Different organic and inorganic ligands on QD surface can have a significant impact on the distribution of the electron density of states, thus further enriching the tunability of QD electrical properties. Lead chalcogenide QDs with different ligands can greatly modulate the carrier density and tune-up energy landscape alignment, which is complementary for bandgap tunability, thus forming a type-II heterojunction. More strikingly, other critical parameters including mobility, lifetime, and the corresponding diffusion length also present facile tunability with different surface ligands. The diffusion length of lead chalcogenide QDs reaches the scale of ~10² to 10³ nm, significantly higher than that of the organic counterparts.⁵⁰ With these benefits, lead chalcogenide QD materials as the rising star, have made rapid progress during the past decade with the power conversion efficiency (PCE) in the range from ~3% to over 15% (Fig. 1b and 2c–e).

In addition, perovskite QDs have drawn great research interest due to their strong and sharp emission, high mobility, low exciton binding energy, high defect tolerance, and great phase stability (Fig. 2d).^{51–53} Moreover, the bandgap and absorption of perovskite QDs can also be significantly tuned with different halogen elements, mainly including I[–], Br[–], and Cl[–]. Therefore, perovskite QDs exhibit the broad absorption covering the whole visible light range, which is critical for high-performance solar cells. In addition, the high defect tolerance and photoluminescence quantum yields also endow great potential for perovskite QDs to develop them as promising candidates for future photovoltaic devices. More strikingly, perovskite QDs also present a superior mobility of ~1–100 cm² V^{–1} s^{–1} and a high diffusion length of ~10³ to 10⁴ nm, which can deliver efficient carrier transport for solar cells. With these benefits, perovskite QDSCs have witnessed great advances, with the PCE increasing from 10.77% to over 16.0% in the past few years.^{18,51}

Despite the great advances, the high toxicity of Pb-based QD materials have raised great concerns in the electronic community, which has offered a chance for the exploration of eco-friendly alternatives. Ecofriendly and earth-abundant QDs have emerged as promising materials for photovoltaic devices. The star nontoxic AgBiS₂ QDs have seen a dramatic surge due to their promising opto-electronic properties, including broad absorption range, high absorption coefficient, favorable energy landscape, and great ambient stability.^{54–57} With joint efforts, the photovoltaic performance of AgBiS₂ QDSCs has been improved to over 9.0% in 2022 (Fig. 1b).^{58,59} In addition, other promising ecofriendly QDs also hold great potential in photovoltaics, photodetectors, and photoelectrochemical cells.^{60–62} On the other hand, high efficiency, long-term stability, and low cost all play the major role in the large-scale applications of



Long Ye has been a Professor at the School of Materials Science & Engineering of Tianjin University since October 2019. He received his PhD degree from the Institute of Chemistry, Chinese Academy of Sciences in 2015. From 2015 to 2019, he was a postdoctoral researcher and later promoted to research assistant professor at the Department of Physics, North Carolina State University. His current interests include organic/hybrid solar cells and energy conversion-related applications.

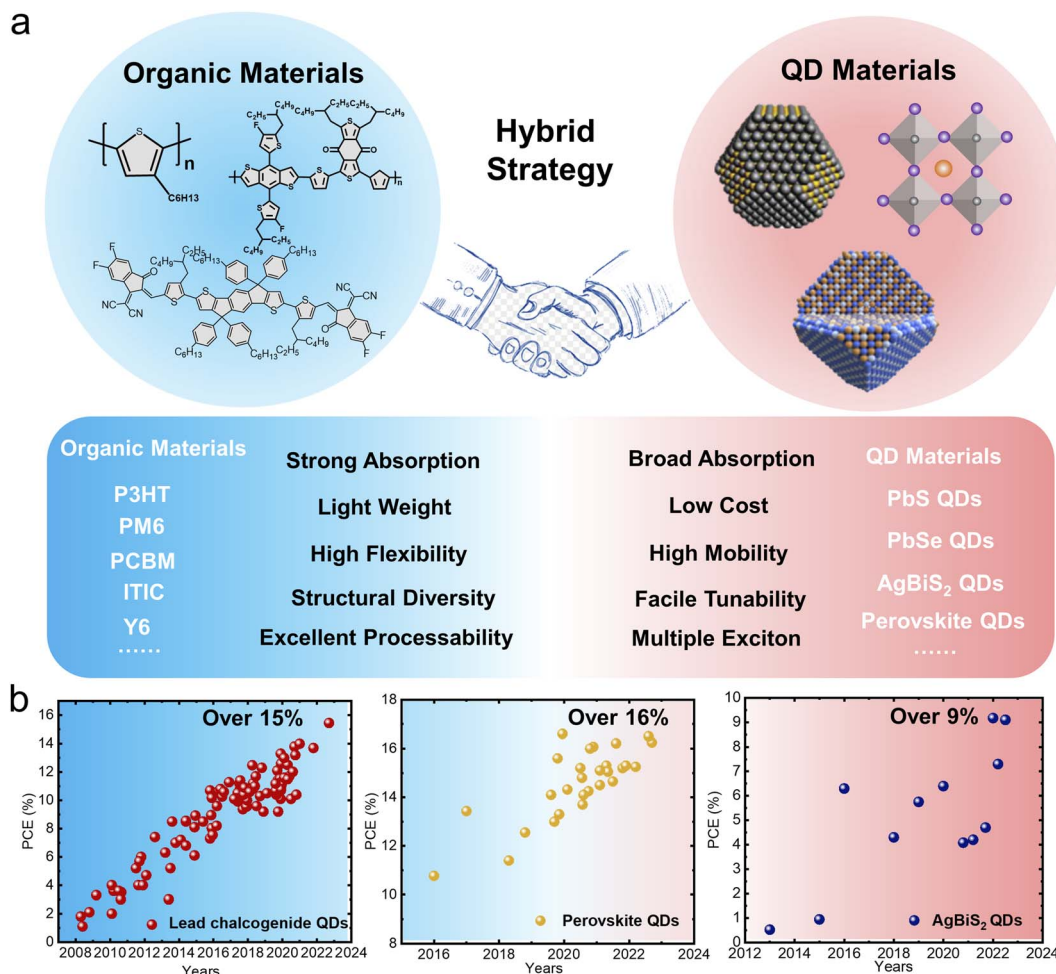


Fig. 1 (a) The advantages of organic and QD photovoltaic materials (Organic materials: P3HT, PM6 and IEICO-4F; QD materials: PbS QDs, perovskite QDs, and AgBiS₂ QDs). (b) The progress of hybrid solar cells with three promising QD materials, namely, PbS QDs, perovskite QDs, and AgBiS₂ QDs.

emerging photovoltaics. With regard to the distinct merits of OSCs and QDSCs, hybrid strategy holds promising potential to be leveraged for a win-win situation, in which OSCs can further improve the performance and stability, while QDSCs can propel rapid progress in the power conversion efficiency.

With the unique benefits of QD materials, hybrid QD/organic solar cells have witnessed promising progress with the markedly increased efficiency and stability. Since no prior reviews has been exclusively dedicated to this important frontier, it is quite timely to summarize the current status, strategies, and future perspectives. Herein, we presented a comprehensive and critical review of state-of-the-art hybrid solar cells with the goal of advancing the large-scale applications of the emerging solution-processing devices. Accordingly, we firstly discuss in detail the working principles of hybrid solar cells and highlighted the combined support for high-performance and high-stability hybrid photovoltaics. Subsequently, QD passivation with organic ligands is further overviewed, aiming to provide critical insights into further enhancing the performance of QDSCs. Then, the in-depth discussion on the device structure of hybrid solar cells and the corresponding research efforts,

mainly including bulk-heterojunction, bilayer, and tandem structure, is given. More importantly, we further present the remaining open challenges and offer our insights into the corresponding research directions for the further performance and stability improvement of hybrid solar cells.

2. Working principles

Prior to discussing QD and organic hybrid strategies in detail, we firstly present the elaboration of the fundamentals for the combination of QDs and organics. For QD passivation, short ligands are the generally recognized prerequisite for QD coupling, therefore enhancing carrier hopping and mobility to advance QD photovoltaic performance. In addition, QD stability with organic short ligands is the other critical issue for solar cell processing. When in solution, organic ligands can increase the QD solubility, while in the films, organic ligands can improve the QD stability from water and oxygen in the air. Moreover, organic ligands can simultaneously reduce the trap density, which is favorable for the carrier transport and the improvement of the open-circuit voltage (V_{oc}) for QD solar cells.⁶⁴⁻⁶⁶

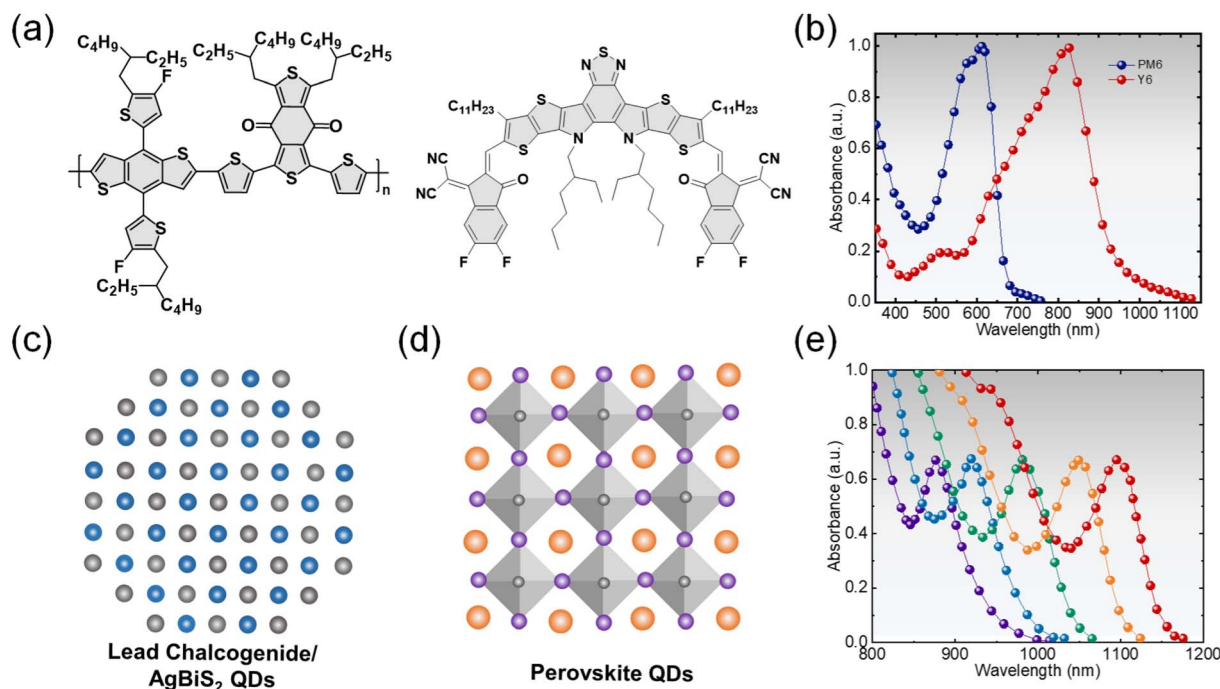


Fig. 2 Optical and electrical properties of organic and QD photovoltaic materials. (a and b) Molecular structure and absorbance spectra of the PM6 donor and the Y6 acceptor. (c) Schematic of the structure of lead chalcogenide/AgBiS₂ QDs. (d) Schematic of the structure of perovskite QDs. (e) Absorbance spectra for PbS QDs with the increase in QD size. (b) Reproduced with permission from ref. 38 Copyright 2019, Elsevier. (e) Reproduced with permission from ref. 63 Copyright 2011, American Chemical Society.

We proceed to discussing the basic principles of hybrid QD/organic solar cells with bulk heterojunction, bilayer, and tandem structure from optical, electrical, and morphological properties. For all the three structures, the complementary absorption of QDs and organics is the essential prerequisite for efficient hybrid solar cells (Fig. 3a). More specifically, high-performance OSCs generally have an absorption cutoff of less than 1000 nm, leaving abundant solar radiation unavailable, which places great restrictions on further performance advancement of this technology.^{67–70} Coincidentally, the facile size-dependent tunability endows lead chalcogenide QDs with the absorption covering the broad range from ultraviolet (UV) to even short-wave infrared. Accordingly, lead chalcogenide QDs can offer great complementary absorption with organic photovoltaic materials. In addition, the notorious absorption valley of lead chalcogenide QDs stemming from quantum confinement is recognized as one of the major roadblocks for their further efficiency improvement.^{71–73} Fortunately, a large number of organic photovoltaic materials can exhibit the desirable absorption peak, offsetting the valley from lead chalcogenide QDs, which is expected to deliver superior photovoltaic performance for QDSCs. Moreover, the instability of organic photovoltaic materials under UV illumination can be significantly relieved with lead chalcogenide QD materials, which generally present the favorable UV stability.

For electrical properties, bulk heterojunction and bilayer structure generally require the favorable type-II energy level alignment for efficient electron and hole transport, which is the main prerequisite for high-performance hybrid solar cells

(Fig. 3b). Nevertheless, a tandem structure presents the loose requirement of energy landscape between QD and organic materials due to the use of electron and hole transport layer (ETL or HTL) for efficient carrier extraction. Crucially, high-performance hybrid solar cells with bulk heterojunction generally raise the requirement of the balanced electron and hole transports to reduce carrier recombination, therefore significantly enhancing photovoltaic performance. To this end, the comprehensive matching between QD and organic photovoltaic materials must be fulfilled such as mobility, carrier density and energy level difference, which jointly leads to the balanced carrier transport. Moreover, perovskite QDs with direct exciton dissociation and high mobility can greatly enhance carrier transport and the corresponding photovoltaic performance when introduced into organic bulk heterojunction.^{74–76} For bilayer structure, QD/organic heterojunction generally presents only one leading carrier transport, which requires significantly higher electron or hole mobility and carrier density, with the aim to build the sufficient dissipation zone for fast carrier extraction.

Similar to the requirements of electrical properties, high-performance hybrid solar cells also have some combination principle of QDs and organics in terms of morphology, especially for bulk heterojunction and bilayer structures. As established from efficient OSCs, bulk-heterojunction solar cells generally require favorable mixing or phase separation for two or multiple materials, which is also available for QD:organic heterojunction (Fig. 3c). Nevertheless, lead chalcogenide QDs with different ligands exhibit tunable surface energy, which is

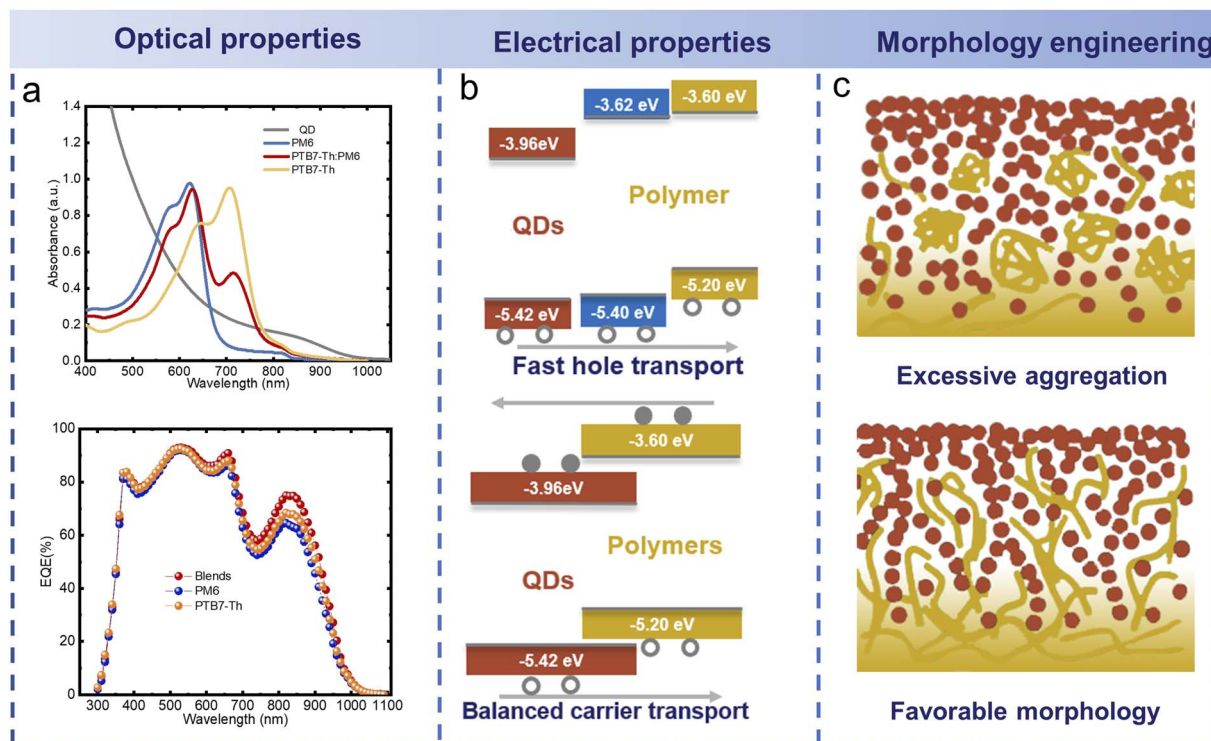


Fig. 3 Basic principles of hybrid QD/organic solar cells in terms of optical, electrical, and morphology properties. (a) Complementary absorption of QDs and organics for bulk heterojunction, bilayer, and tandem structure (red and yellow curves are for different organics, and the brown curve is for QDs). (b) Energy level alignment of QD/polymer heterojunction for bilayer structure (top) and bulk heterojunction (bottom). (c) Morphology engineering for QD/polymer bulk-heterojunction. (a) Reproduced with permission from ref. 77 Copyright 2022, Wiley. (c) Reproduced with permission from ref. 78 Copyright 2015, Wiley.

expected to achieve good matching with organic photovoltaic materials to achieve favorable phase separation. Nevertheless, it is worth noting that when seeking out QD and organic pairs, we must present the overall consideration of complementary absorption, energy landscape alignment, and favorable morphology. In addition, recent reports have revealed that monolayer morphology also plays a critical role in carrier transport, especially for organic ETLs and HTLs, which is greatly affected by aggregated structure and the corresponding morphology.

On the whole, bulk-heterojunction and bilayer structures have more requirements in terms of optical properties, electrical properties, and morphology of QDs and organics, while the tandem structure presents the loose requirement, with only attention to the optical properties. Except for the general requirements for optical, electrical, and morphological properties, there is another critical principle that the introduced organics cannot destroy QD passivation, especially for small molecule photovoltaic materials, which may displace the original QD ligands, leading to the increased traps and therefore marked reduction of photovoltaic performance.

3. QD passivation

Organic ligands have witnessed a long history for the passivation of QDs, which are generally synthesized with long ligands

for stability and solubility, *e.g.*, oleic acid and oleyl amine.^{79,80} Nevertheless, long ligands have blocked carrier hopping, which is the prerequisite for photovoltaic applications. Therefore, worldwide research efforts have been devoted to developing available short ligands displacing primitive long ligands to increasing QD coupling. We summarize the greatly used organic ligands for lead chalcogenide QDs and perovskite QDs in Fig. 4a and b. This review only discussed the promising passivation of lead chalcogenide and perovskite QDs with organic ligands. It can be clearly seen that more research efforts have been devoted to developing various organic ligands for high-performance perovskite QDs, which have recently aroused worldwide attention over lead chalcogenide QDs.^{81–83}

3.1 Lead chalcogenide QD passivation

There have emerged many pioneering reviews on PbS QD passivation with organic short ligands.^{40,65,84} Here, we mainly present a brief discussion on the recent progress of organic ligands for superior surface passivation. Organic short ligands, such as 1,2-ethanedithiol (EDT),^{85–87} 1,4-benzenedithiol (BDT),⁸⁸ and 3-mercaptopropionic acid (MPA),^{89–91} generally cannot offer perfect passivation for QDs, leading to the moderate photovoltaic performance. When exposed to air, oxygen will erode QDs, resulting in increased defect state, which affects their photovoltaic performance. Therefore, organic ligands gradually lose their competitiveness compared with promising halide ligands.

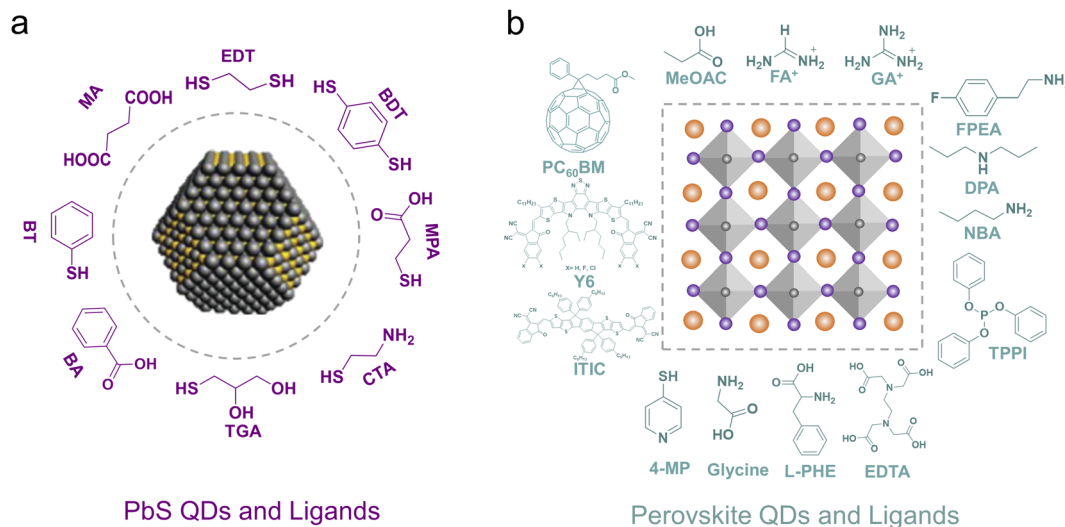


Fig. 4 QD passivation with organic short ligands. (a) PbS/Se QDs with common organic ligands. (b) Perovskite QDs with different kinds of organic ligands.

Despite imperfect passivation, QDs with organic ligands have been developed as favorable HTL, which have endowed further success in the field of lead chalcogenide QDSCs. Even to date, QDs with EDT ligands still demonstrate the most popular HTLs for high-performance QDSCs.^{73,92,93} Nevertheless, EDT ligands have introduced some negative issues, *e.g.*, notorious pungent odor, pinhole stemming from their strong reactivity, passivation destruction of the active layer, and tedious solid-state ligand exchange (SSLE).^{94–96} In this regard, Sargent's group has contributed considerably to address this challenge. Their recent work replaced conventional EDT ligands with nontoxic malonic acid (MA), which has nearly no impact on the bottom layer, due to the moderate reactivity (Fig. 5a and b).⁹⁷ With this benefit, QDs with MA ligands have a champion PCE of 13%, compared to 12.2% with EDT ligands. Despite the significant benefit, this process still cannot be free of SSLE, which has placed great restrictions on its commercial applications. With regard to this challenge, they further introduced benzoic acid for QD passivation to develop weakly-polar QD inks, which was compatible with the processing of QD inks with iodine ligands, therefore bridging the gap for large-scale applications of QDSCs.⁹⁸

Despite the leading role of halide ligands in PbS QD passivation, there still exist quite a few defects on the QD surface, which are unfavorable for the further improvement of photovoltaic performance.^{39,100} On account of this issue, Sargent's group, Konstantatos' group, and Ma's group have developed hybrid QD passivation with organic and halide ligands, which have exhibited significant improvement in the photovoltaic performance.^{99,101,102} Konstantatos' group¹⁰¹ and Ma's group¹⁰² both employed iodine and MPA ligands to passivate lead chalcogenide QDs, which presented the marked enhancement of V_{oc} , indicating more perfect QD passivation. Recently, Sargent's group has delivered a facile hybrid passivation strategy with iodine and cysteamine ligands, therefore developing p-type QD inks, which lead to the markedly increased

photovoltaic performance (Fig. 5c).⁹⁹ With this benefit, they further employed a bulk homojunction with the mixing of n-type and p-type QD inks, which can enable the thick enough QD active layer for solar radiation harvesting, therefore leading to the simultaneous improvement of V_{oc} and short-circuit current (J_{sc}). With these successes, we can expect that organic ligands will still play a critical role in the progress of lead chalcogenide QDSCs.

3.2 Perovskite QD passivation

Perovskite QDs have drawn increasing attention due to their high photoluminescence quantum yield (PLQY), sharp emission, high mobility, high defect tolerance, and great phase stability.^{82,103,104} With joint efforts, perovskite QDSCs have witnessed rapid progress with a certified PCE of 16.6%,¹⁸ significantly higher than that of the PbS QD counterparts. Generally, the hot injection method was employed to prepare high-quality perovskite QDs with long ligands,^{105–107} *e.g.*, oleic acid and oleyl amine, which have blocked dot-to-dot carrier transport. To counter this issue, various short ligands have been developed for high-performance perovskite QDSCs.^{49,108,109} Luther's group has contributed a lot to introduce the magical ligands methyl acetate (EtOAc) and formamidinium (FA⁺) to replace long oleate and oleyl-ammonium ligands, which have been widely used to develop high-performance perovskite QDSCs.^{51,52} Recently, Ma's group employed cationic guanidinium (GA⁺) to develop a surface matrix on CsPbI₃ QDs, which can deliver significantly enhanced charge mobility and carrier diffusion length.¹¹⁰

Except for the above ligands, we have classified the existing short ligands into three categories, including single-acting-group molecules (*e.g.*, FPEA and DPA),^{114,115} multi-acting-group molecules (*e.g.*, amino acid and EDTA),^{116,117} and organic photovoltaic molecules (*e.g.*, ITIC and Y6).^{118,119} The detailed working mechanism and the corresponding performance have been reviewed in recent years;^{53,120,121} here, we only overview

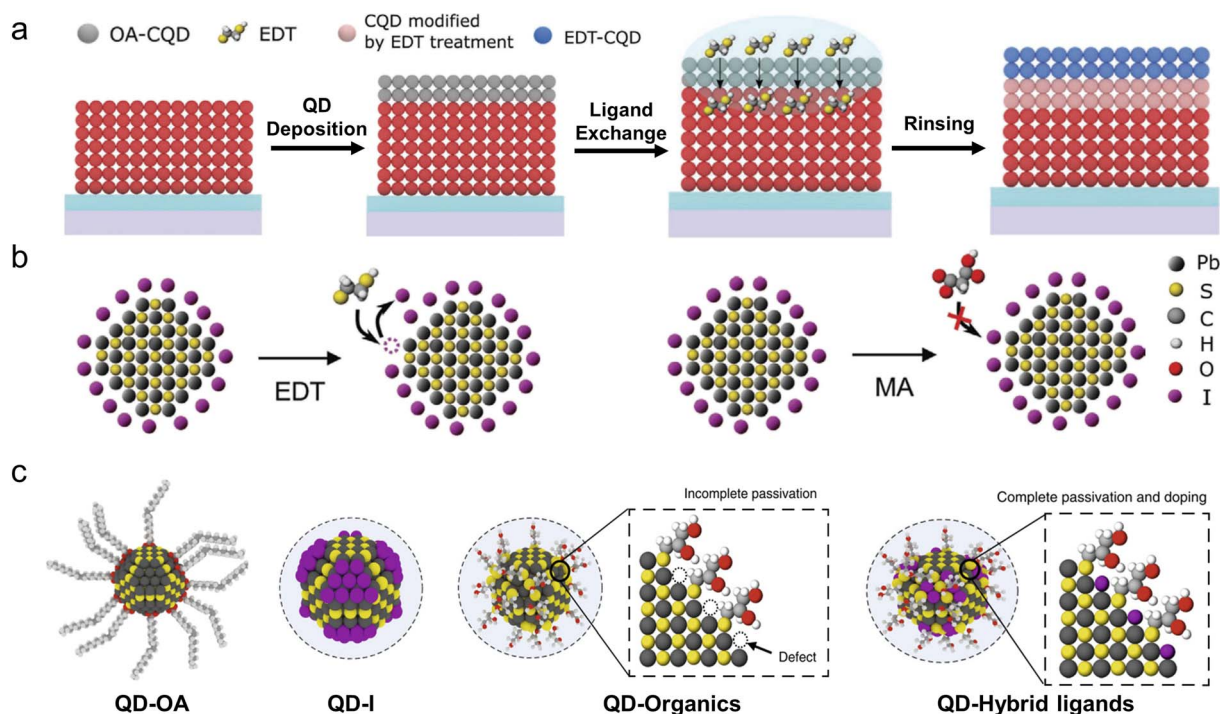


Fig. 5 Lead chalcogenide QD passivation with organic ligands. (a) Conventional QD passivation with EDT ligands, which will destroy the underlying QD active layer. (b) Schematic of QD passivation with EDT and MA ligands. (c) Schematic of QD passivation with single organic ligands and hybrid ligands. (a and b) Reproduced with permission from ref. 97 Copyright 2020, Wiley. (c) Reproduced with permission from ref. 99 Copyright 2020, Springer Nature.

some promising ligands from the detailed treatment process, including the synthesis period, synthetic post-treatment, and solid-state ligand exchange. For instance, Shi *et al.*¹¹¹ proposed the *in situ* ligand treatment during the synthesis of CsPbI₃ QDs using a bifunctional ligand, L-phenylalanine, which can effectively replace original long ligands and offer great passivation due to its substantially improved adsorption energy (Fig. 6a). With this strategy, the developed perovskite QDs exhibited a markedly enhanced solution stability and the corresponding QDSCs presented higher photovoltaic performance from 13.6% to 14.6% (Fig. 6b). Recently, Jia *et al.*¹¹² developed a surface matrix curing strategy to passivate the iodide vacancies of CsPbI₃ QDs during the period of synthetic post-treatment (Fig. 6c). Through the nucleophilic substitution reaction of *tert*-butyl iodide (TBI) and nucleophile trioctylphosphine (TOP), sufficient iodide ions can be produced to provide the significantly improved surface passivation and higher I/Pb ratio (Fig. 6d). With this benefit, the treated CsPbI₃ QDSCs can achieve a record PCE of ~16.2%, markedly higher than the control (~13.2%). More strikingly, the nucleophilic substitution reaction for the release of iodine ions can inspire more research efforts for great QD passivation.

In addition, solid-state ligand exchange has aroused more research efforts owing to its great robustness for various organic ligands.^{122–124} For instance, Wang *et al.*¹¹³ recently reported that triphenyl phosphite (TPPI) ligands can effectively passivate the surface of CsPbI₃ QDs during solid-state ligand exchange (Fig. 6e). The developed QD films exhibited two-fold

improvement, balancing the carrier transport, which can enable high-performance QD solar cells with a markedly improved PCE of 15.2% over the control (Fig. 6f). Furthermore, more organic short ligands (*e.g.*, EDTA, PEAI, and DPA) have been successfully employed to provide perfect QD passivation through solid-state ligand exchange.^{115,116,125} We have summarized the performance of perovskite QDSCs with different organic ligands in Table 1.

4. Hybrid device structure

On account of the complementarity of QDSCs and OSCs, continuous research efforts in the community have been devoted to the QD and organics hybrid strategy.^{132–134} Early research mainly focused on the performance improvement of solar cells with PbS QD:organic bulk-heterojunction. Furthermore, recent research efforts have been devoted to the development of hybrid perovskite QD:organic bulk-heterojunction, which may offer an additional opportunity for further performance breakthrough. Subsequent hotspots have shifted to bilayer and tandem structures with the aim to simultaneously enhance the efficiency and stability of hybrid QD/organic solar cells. To date, hybrid QD/organic solar cells have presented the record PCEs of 16.6%, 14%, and 13.7% for bulk-heterojunction, bilayer, and tandem structures, respectively.^{135–137} In this section, we present a detailed discussion on hybrid QD and organic solar cells including bulk heterojunction, bilayer structure, and tandem structure. The chemical structures and

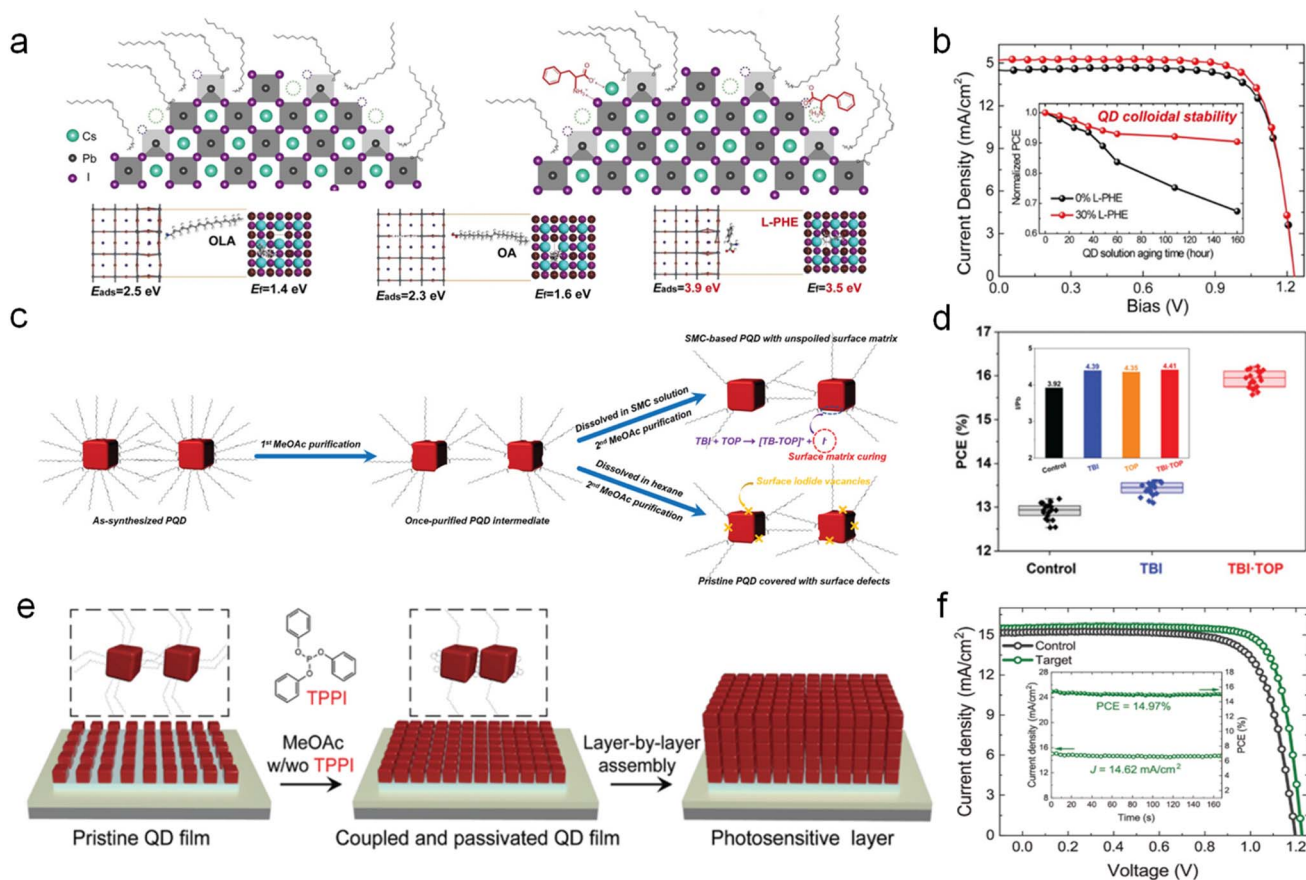


Fig. 6 Perovskite QD passivation with organic ligands. (a) *In situ* QD passivation with L-phenylalanine ligand. (b) J - V curves and solution stability of the developed QDs. (c) Schematic of QD passivation with a surface matrix curing strategy. (d) Photovoltaic performance and I/Pb ratio of the developed QDs. (e) Schematic of QD passivation during solid-state ligand exchange. (f) J - V curves and the steady power output of the developed QDSCs. (a and b) Reproduced with permission from ref. 111 Copyright 2020, Wiley. (c and d) Reproduced with permission from ref. 112 Copyright 2021, The Royal Society of Chemistry. (e and f) Reproduced with permission from ref. 113 Copyright 2021, Wiley.

device structure in hybrid QD and organic solar cells are given in Fig. 7 and 8.

4.1 Bulk-heterojunction

4.1.1 Lead chalcogenide QD:organic blends. Lead chalcogenide QDs were firstly introduced into organic matrixes as the sensitizer to harvest short-wave infrared radiation with bulk heterojunction.^{138–142} Nevertheless, the early hybrid QD:organic solar cells can only deliver the photovoltaic efficiency less than 0.1%, which is mainly attributed to imperfect QD passivation and the lack of understanding on the working principles of QD:organic heterojunction.^{143–145} With the deepening of the understanding on carrier transport of hybrid heterojunction, fast electron and hole transports were confirmed between polymers and QDs with short ligands.^{146–150} Benefiting from continuous efforts, the performance of hybrid QD:organic solar cells has witnessed rapid progress within a few years. Due to the simple synthesis and low cost, P3HT has proved to be the early popular polymer with QDs; however, it presents a moderate PCE, mainly due to the absorption mismatch of the two materials and the driving lack from the low energy landscape

difference.^{147,148,151,152} With EDT ligands from SSLE, hybrid QD:P3HT solar cells can only present a champion PCE of $\sim 1\%$, while it can reach over 3% for QDs with BDT ligands, which still cannot eliminate the use of the tedious SSLE process.¹⁵³ Moreover, Nguyen *et al.* recently designed a block copolymer poly(3-hexylthiophene)-*b*-polystyrene, which can be blended with P3HT and QDs, leading to the further efficiency improvement to $\sim 4.9\%$, which is the champion PCE for hybrid solar cells with P3HT.¹⁵⁴

To maximize solar energy harvesting, complementary absorption remains one of the critical requirements. To address this challenge, polymers with red-shifted absorption have been introduced to further enhance the photovoltaic performance of hybrid solar cells. Seo *et al.* employed the low-bandgap polymer PDTPBT blend with QDs to develop hybrid solar cells, delivering a champion PCE of $\sim 3.78\%$, which does not outperform that with P3HT. This can be attributed to the imperfect passivation of EDT ligands, as revealed above (Fig. 9a and b).¹⁵⁵ With regard to this issue, Ma's group have exploited the moderate-reactivity BDT for ligand exchange, and they achieved a record PCE of 5.5% for hybrid QD:PDTPBT solar cells with further morphology

Table 1 The performance of QDSCs with organic short ligands

	Solar cell structure	V_{oc} (V)	J_{sc} (mA cm ⁻²)	FF (%)	PCE (%)	Ref.	
Lead chalcogenide QD	ITO/TiO ₂ /PbS-EDT QD/Au	0.59	8.9	55.9	2.94	126	
	ITO/PbS-BDT QD/LiF/Al	0.46	19.3	58.0	5.2	88	
	ITO/TiO ₂ /PbS-MPA QD/MoO ₃ /Au/Ag	0.48	31.0	52.0	7.3	127	
	ITO/ZnO/PbS-PbI ₂ QD/PbS-MPA QD/Au	0.64	23.9	71.0	10.9	128	
	ITO/ZnO/PbS-PbX ₂ QD/PbS-EDT QD/Au	0.65	28.7	65.0	12.2	97	
	ITO/ZnO/PbS-PbI ₂ QD/PbS-MPA + EDT QD/Au	0.63	25.3	66.8	10.4	95	
	ITO/ZnO/PbS-PbX ₂ QD/PbS-MA QD/Au	0.64	29.1	70.0	13.0	97	
	ITO/ZnO/PbS-ZnI ₂ + MPA QD/PbS-EDT QD/Au	0.66	24.5	61.3	9.9	101	
	ITO/ZnO/PbS-PbX ₂ + MPA QD/PbS-EDT QD/Au	0.61	27.4	66.8	11.2	102	
	ITO/ZnO/PbS-PbX ₂ :PbS-CTA QD/PbS-EDT QD/Au	0.65	30.2	68.0	13.3	99	
	Perovskite QDs	FTO/TiO ₂ /CsPbI ₃ -4-MP/PTAA/MoO ₃ /Ag	1.25	14.32	79.0	14.25	129
		FTO/TiO ₂ /CsPbI ₃ -EtOAc/Spiro-OMeTAD/MoO ₃ /Al	1.23	13.47	65.0	10.77	51
		FTO/TiO ₂ /CsPbI ₃ -FAI/Spiro-OMeTAD/MoO ₃ /Al	1.16	15.25	76.63	13.43	52
FTO/TiO ₂ /CsPbI ₃ -TPPI/PTAA/MoO ₃ /Ag		1.20	15.2	74.5	13.55	113	
FTO/TiO ₂ /CsPbI ₃ -GASCN/PTAA/MoO ₃ /Ag		1.25	15.85	76.7	15.2	110	
FTO/TiO ₂ /CsPbI ₃ -DPA/PTAA/MoO ₃ /Ag		1.24	15.84	75.5	14.9	115	
FTO/TiO ₂ /CsPbI ₃ -FPEA/PTAA/MoO ₃ /Ag		1.28	15.4	74.7	14.65	125	
ITO/SnO ₂ /CsPbI ₃ -TBI/TOP/Spiro-OMeTAD/Ag		1.27	17.71	72.0	16.2	130	
FTO/TiO ₂ /CsPbI ₃ -NaOAc/Spiro-OMeTAD/Ag		1.21	14.7	69.6	12.4	131	
FTO/TiO ₂ /CsPbI ₃ -PEAI/Spiro-OMeTAD/Ag		1.23	15.3	74.8	14.1	114	
ITO/SnO ₂ /CsPbI ₃ -EDTA/Spiro-OMeTAD/Ag		1.23	17.51	71.0	15.25	116	
ITO/SnO ₂ /CsPbI ₃ -glycine/Spiro-OMeTAD/Ag		1.22	17.66	63.4	13.66	117	

modulation and device optimization (Fig. 9c and d).⁷⁸ Moreover, they proceeded to seek out six polymers with different absorption ranges to blend with lead chalcogenide QDs, and the corresponding devices delivered the champion PCE of ~4.3% with the promising polymer PDBT, which has presented complementary absorption with QDs.¹⁵⁶ Despite the progress, all the above efforts still cannot fulfill the potential of hybrid solar cells due to the low performance and complex processing stemming from the unfavorable SSLE process, which may destroy the morphology of the hybrid QD:organic heterojunction and simultaneously increase the complexity.

With the rapid progress of lead chalcogenide QD inks, more and more research efforts have been devoted to the more promising passivation with halide ligands, which can also offer ideal building blocks for high-performance hybrid QD:organic solar cells. Nevertheless, blending organics and QD inks still remains an open challenge, which is mainly attributed to most high-performance polymers that can only be dissolved in non-polar solvents, incompatible with the highly polar QD inks. To address this issue, Lu *et al.* developed a facile strategy to blend PbS QDs and the polymer (Si-PCPDTBT) with the aid of *n*-butylamine.¹⁵⁷ Accordingly, the hybrid solar cells can offer a broad spectral response into the NIR, resulting in a PCE of 4.8% under AM 1.5G illumination and deliver favorable carrier transport between PbS QD and Si-PCPDTBT (Fig. 9e). Despite the progress, compared with advanced phase transfer ligand exchange (PTLE), the process only involves the simple post-deposition treatment with PbI₂ ligands, which cannot completely replace the insulating organic ligands, resulting in poor QD passivation and therefore inferior photovoltaic performance. Ongoing research efforts should pay more

attention to develop the strategy of blending organics and PbS QDs with halide ligands.

4.1.2 Perovskite QD:organic blends. Despite the end capping of long ligands, perovskite QDs show a weak dependence on the SSLE process owing to their large size and high mobility. Moreover, the moderate treatment during the SSLE process (generally with EtOAc) has little impact on the morphology of organic:QD blending films.^{18,51} On account of these benefits, hybrid perovskite QD:organic solar cells hold great potential for further performance improvement. To advance the performance of perovskite CQSSCs, Xue *et al.*¹¹⁸ introduced conjugated small molecules (ITIC) into perovskite QDs during the ligand exchange process (Fig. 10a). They found that the perovskite QDs and ITIC can form a favorable type-II heterojunction, which can provide an additional drive for effective charge separation. The time-resolved photoluminescence (TRPL) decay profile of the developed QDs with ITIC exhibited the markedly reduced relaxation time, indicating faster carrier transport, which can significantly improve the performance of hybrid QD:organic solar cells to ~13% (Fig. 10b). Similarly, Yuan *et al.*¹¹⁹ recently developed hybrid perovskite QDs:organic solar cells with Y6 series non-fullerene molecules, which can not only enable type-II energy alignment for efficient charge transfer but also reduce the surface defects and energetic disorder of QDs. In addition, Hu *et al.*¹⁵⁸ also introduced fullerene molecule (PC₆₁BM) into perovskite QDs during ligand exchange and found that the CsPbI₃ QD/PCBM heterojunction can enable an energy cascade for efficient charge transfer and mechanical adhesion, and endow high photovoltaic and mechanical performance.

Perovskites QDs can also bring great benefits for the further performance improvement of OSCs. In 2019, Guijarro *et al.*¹⁵⁹

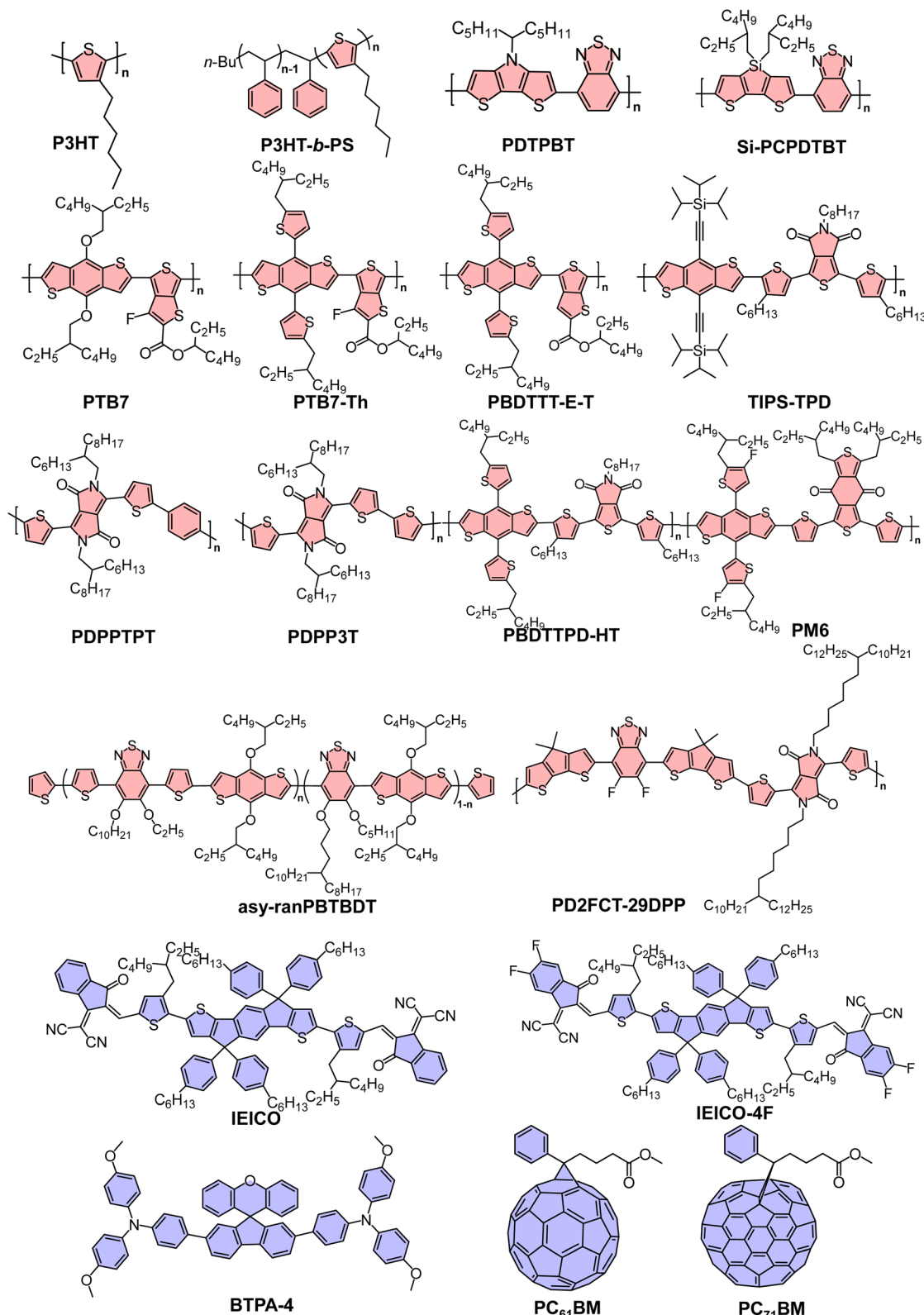


Fig. 7 Chemical structures of some representative polymers and small molecules in hybrid QD and organic solar cells.

successfully introduced CsPbI₃ QDs into a donor-acceptor (PTB7-Th:PC₇₁BM) bulk heterojunction and demonstrated that perovskite QDs can improve exciton separation in the acceptor

phase and reduce recombination, enabling the markedly improved photovoltaic performance (10.84% vs. 7.94%). In addition, a recent work by Zhan's group¹⁶⁰ has demonstrated

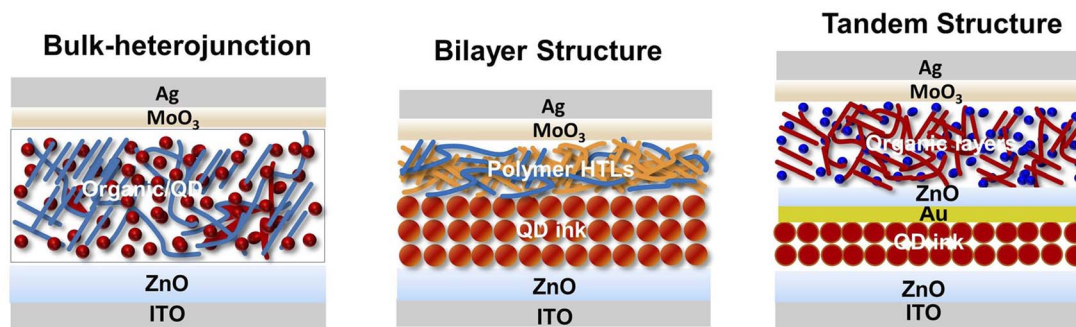


Fig. 8 Device structures for hybrid QD and organic solar cells, including bulk-heterojunction, bilayer, and tandem structures.

that the incorporation of perovskite QDs into organic bulk heterojunction can dramatically increase the energy of the charge transfer state, resulting in near-zero driving force and improved V_{oc} (Fig. 10c). Even at near-zero driving force, hybrid QD: organic solar cells can still exhibit efficient charge generation than the control due to the formation of a cascade band structure and the increased molecular ordering. Moreover, the high dielectric constant of the perovskite QDs screened the coulombic interactions and thereby reduced charge recombination, which can further improve the performance of hybrid solar cells. With the benefit of perovskite QDs, the developed hybrid solar cells with PM6:Y6 blends can achieve a markedly improved PCE of 16.6% over the control (Fig. 10d). Despite the progress, more research efforts are encouraged to develop

promising hybrid QD:organic solar cells, which may offer an additional avenue for the further performance breakthrough of OSCs.

We proceed to discuss the existing challenges for hybrid QD:organic solar cells and the promising route for further performance improvement. For lead chalcogenide QD:organic hybrid systems, the main challenge is the inferior photovoltaic performance, mainly stemming from the essential use of post-treatment for ligand replacing, which will destroy the hybrid QD:organic film due to the kinetically-hindered process. Moreover, the developed co-dissolution strategy still exhibits the inferior photovoltaic performance, which can be attributed to the poor QD passivation from the simple postdeposition treatment.¹⁵⁷ Accordingly, the developed high-polarity QD inks

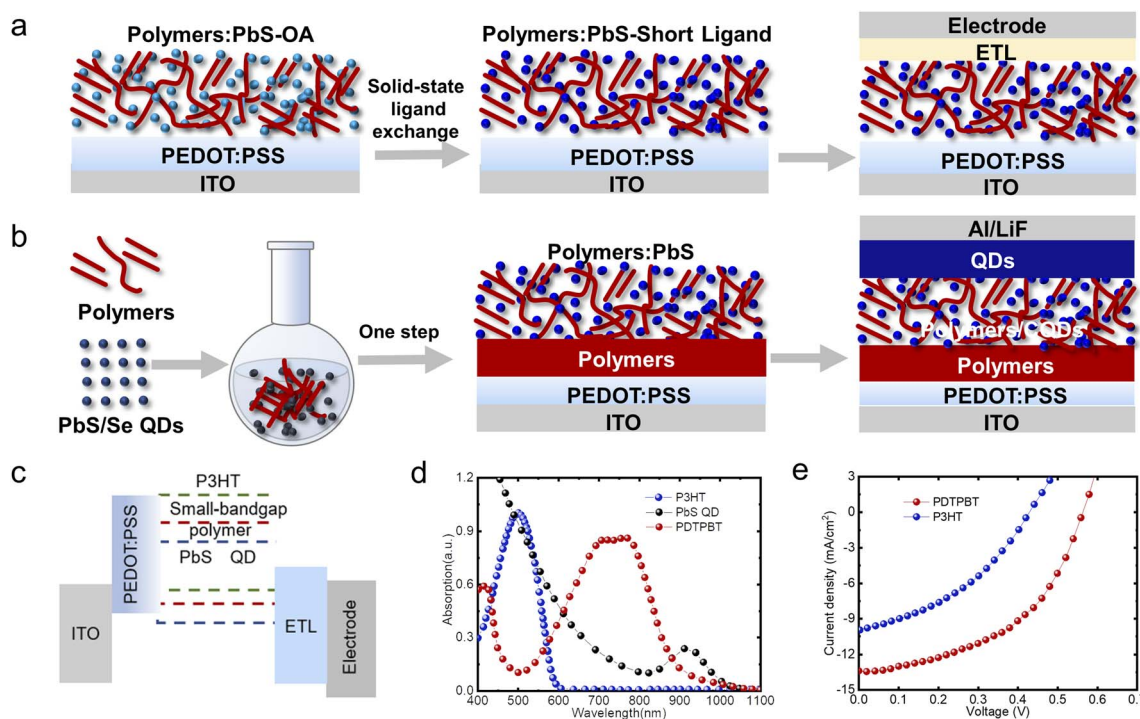


Fig. 9 Hybrid lead chalcogenide QD: organic solar cells with bulk heterojunction. (a and b) The processing of hybrid QD:organic solar cells for SSLE and directly mixed methods, respectively. (c) Schematic of energy level alignment of polymer and QDs. (d) Absorption spectrum of QDs and polymers with/without complementarity. (e) Photovoltaic performance of hybrid QD:polymers solar cells with P3HT and PDTBPB. (c–e) Reproduced with permission from ref. 155 Copyright 2011, Wiley.

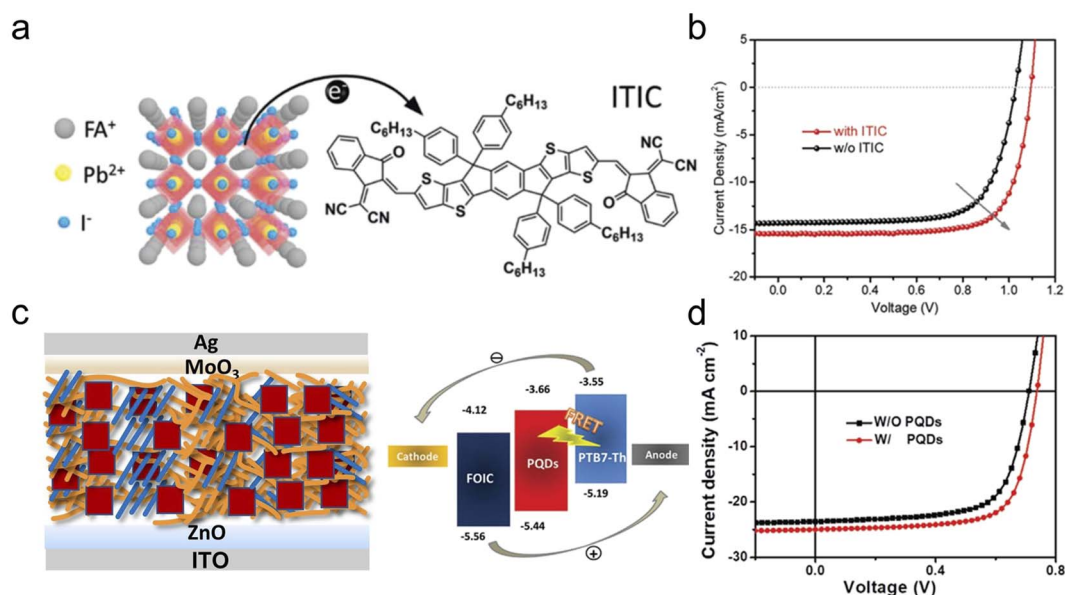


Fig. 10 Hybrid perovskite QD:organic solar cells with bulk heterojunction. (a) Schematic diagram of charge transport between perovskite QDs and ITIC. (b) J - V curves of the perovskite QDSCs with ITIC molecule. (c) Device structure of hybrid perovskite QD:organic solar cell and energy level alignment between organics and perovskite QDs. (d) J - V curves of OSCs with perovskite QDs. (a and b) Reproduced with permission from ref. 118 Copyright 2019, Wiley. (c and d) Reproduced with permission from ref. 160 Copyright 2020, Wiley.

may emerge as promising candidates for hybrid QD:organic solar cells, but it is highly essential to modulate the polarity of QD inks for high miscibility. The pioneering work by Sargent's group may shed further light on the development of non-polar QD inks, which are expected to deliver further success for hybrid QD:organic solar cells.^{98,161} For perovskite QD:organic hybrid system, more attention should be paid to develop better passivated QDs, which may further enhance the performance of hybrid perovskite QD:organic solar cells. In addition, further understanding of the morphology modulation for the hybrid QD:organic film is the prerequisite for fast carrier transport and, therefore, high photovoltaic performance. The well-developed OSC bulk heterojunction may offer promising inspirations the morphology control, *e.g.*, miscibility analysis with Flory-Huggins interaction parameter.^{13,70,162}

4.2 Bilayer structure

Compared to the preparation limit of bulk heterojunction, hybrid QD:organic solar cells based on the bilayer structure have been demonstrated to hold great potential for further performance enhancement. According to the main function of organic photovoltaic materials, QD/organic bilayer structures can be divided into three types: (I) QDs for light absorption and organics for HTLs, (II) QDs and organics coequally for light absorption, and (III) organics, mainly for light absorption. On the whole, organic photovoltaic materials for HTLs (type I) have dominated the investigation of the bilayer structure owing to their facile processing and efficient hole extraction. At present, the performance of type II and III has not been fully demonstrated due to less research efforts in the field. Nevertheless, their great potential in enhancing the photovoltaic performance

and stability may offer an additional opportunity for organic solar cells.

4.2.1 Lead chalcogenide QD/organic structure. For lead chalcogenide QDs, early research efforts on bilayer structure have mainly focused on the existing organic HTLs from well-developed perovskite solar cells, such as PTAA and P3HT, which can only endow the moderate photovoltaic performance with a record PCE of $\sim 7.5\%$.^{163,164} Our recent report demonstrated that nonhalogenated solvent processing can boost the PCE of PbS QD/P3HT hybrid solar cells up to 8.7%, setting a new record for this type of hybrid solar cells.¹⁶⁵ Further investigations have confirmed that the mismatch of energy landscape between QDs and P3HT emerged as the major roadblock in performance improvement. Polymers with low energy level indeed deliver faster hole transport, leading to the further performance increase with PCEs of $\sim 10\%$ for PTB7,¹⁶⁶ $\sim 10.3\%$ for PTB7-Th,¹⁶⁷ 11.2% for PBDB-TF,¹⁶⁸ and 11.5% for PBDTTPD-HT.¹⁶⁷ More strikingly, PBDB-TF HTL recently delivered a high PCE of $\sim 12.8\%$, approaching the record photovoltaic performance in the field, which indicates the great potential of polymer HTLs.¹⁶⁹ Baek *et al.* developed a hydro/oxo-phobic doped organic HTL with robust and outstanding electrical properties, which can protect the underlying PbS layer, deliver a PCE of 11.7%, and retain over 90% of the initial performance after 1 year storage under ambient conditions.⁴³

Except for the existing polymer HTLs, some reports have designed special polymer HTLs for high-performance hybrid solar cells according to the detailed requirement from QDSCs (Fig. 11a). Mubarak *et al.* recently developed a π -conjugated polymer with push-pull structure, including a weakly electron-withdrawing triisopropylsilylethynyl (TIPS) group and the weak donor moiety benzodithiophene for fast hole extraction. The

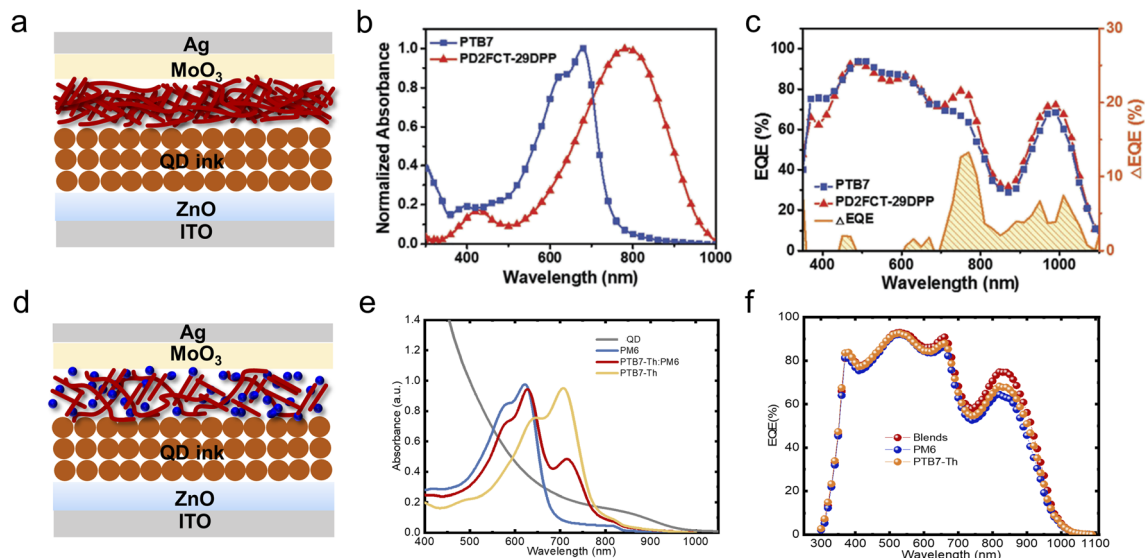


Fig. 11 The device structure and performance of hybrid lead chalcogenide QD/organic solar cells with bilayer structure. (a) Device structure of the hybrid solar cell with single polymer HTL. (b) Absorption spectrum of polymers with/without complementarity for QDs. (c) External quantum efficiency (EQE) spectra of hybrid solar cells with different polymer HTLs. (d) Device structure of the hybrid solar cell with bulk-heterojunction HTL. (e) Absorption spectrum of QDs and organics PBDTTT-E-T and IEICO. (f) EQE spectra of solar cells with/without polymer HTLs. (b and c) Reproduced with permission from ref. 137 Copyright 2020, Wiley. (e and f) Reproduced with permission from ref. 77 Copyright 2022, Wiley.

designed π -conjugated polymer can deliver a champion PCE of 13.03%, significantly higher than that of previously reported polymers.¹⁷⁰ In addition, Kim *et al.* designed a new random polymeric HTL (asy-ranPBTBDT) with the strong π - π stacking face-on orientation and less lateral grain growth compared to asy-PBTBDT, which can reduce charge recombination and enhance device stability. Accordingly, the developed hybrid solar cell exhibited a striking PCE of 13.2% and retained 89% of its initial efficiency after 120 h continuous operation at maximum power point (MPP), while the asy-PBTBDT counterpart can only present a PCE of 11.4% and 71% degradation.¹⁷¹ Moreover, the group proceeded to design a novel DPP-based polymer HTL, PD2FCT-29DPP, with a strong electron accepting moiety, and fluorinated BT to deepen the valence-band level, leading to higher V_{oc} .¹³⁷ The developed polymer formed the favorable vertical aggregation from the strong face-on oriented π - π stacking, which can endow fast vertical charge transport and therefore result in a significantly suppressed bimolecular recombination. Furthermore, the absorption peak near 800 nm of the designed polymer is leveraged for complementary absorption with lead chalcogenide QDs, which can further raise the J_{sc} to over 30 mA cm^{-2} (Fig. 11b and c). Accordingly, the developed hybrid solar cells can achieve an FF of 70.0% and a PCE of 14.0%, which are the champion values in this field.

In a parallel vein, it is well-established that organic acceptors generally exhibit the deep valence-band level, which can be employed to simultaneously enhance light absorption and deepen the whole energy landscape (Fig. 11d-f). Accordingly, Ma's group recently reported an organic bulk heterojunction composed of PTB7-Th blending with various n-type acceptors, which can significantly improve the V_{oc} and J_{sc} hybrid solar cells

(type II).¹⁷² The introduction of fullerene into organic HTLs can improve the interfacial morphology, reduce leakage current and device resistance, and enhance interfacial charge extraction, therefore resulting in the significantly increased V_{oc} and J_{sc} , which eventually endowed a high PCE of 12.02%. In addition, another pioneering work on the QD/organic type II structure reported that the small molecule acceptor, IEICO, can not only offer complementary absorption with lead chalcogenide QDs but also facilitate carrier transport between QDs and organic HTLs, which jointly contributed to the markedly increased J_{sc} .¹⁷³ Therefore, the developed hybrid solar cells exhibited a champion PCE of $\sim 13.1\%$, significantly higher than that of organic-only (8.0%) and QD-only (10.4%) counterparts. More strikingly, the developed hybrid organic:QD solar cells can retain over 90% of the initial PCE even after 3500 h storage under ambient conditions without encapsulation and retain over 80% of the initial performance after 150 h continuous MPP operation, significantly outperforming organic-only and QD-only devices by a factor of 100 and 5, respectively. This superior photostability mainly stems from the high-energy UV photons that are absorbed in the bottom QD film before reaching the organic bulk heterojunction, therefore markedly reducing the photodegradation mechanism of OSCs.

Recently, our group developed a facile polymer blending strategy for high-performance hybrid QD and organic solar cells with enhanced V_{oc} and J_{sc} .^{77,174,175} We developed the facile brominated polythiophenes for the further breakthrough of QD/polythiophene solar cells with type I structure.¹⁷⁵ The energy level of polythiophene was markedly reduced, which can enable a favorable energy landscape, fast carrier transport, and less charge recombination. Accordingly, the photovoltaic performance of QD/polythiophene solar cells was boosted from 8.7%

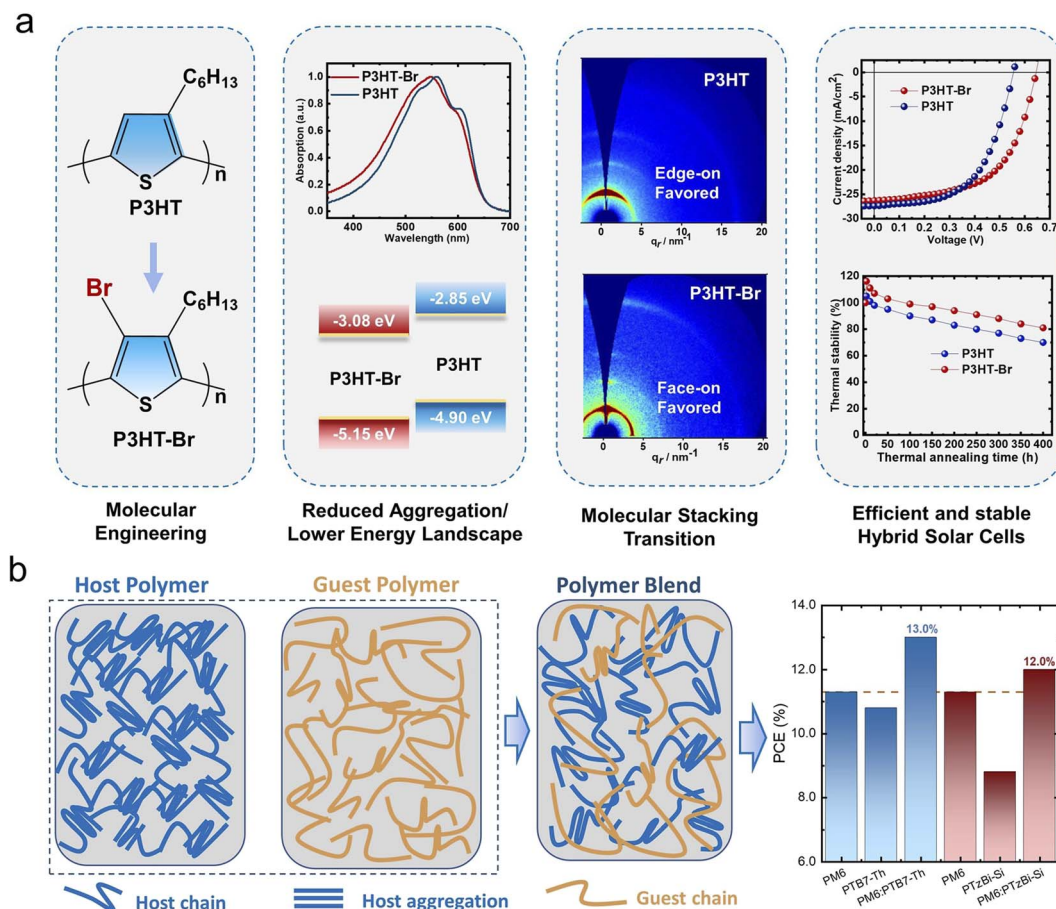


Fig. 12 (a) Structure–property relationships for high-performance and stable hybrid QD/polythiophene solar cells. (b) Schematic of the morphological superiority of the polymer blend in the QD/polymer hybrid solar cells. (a) Reproduced with permission from ref. 175 Copyright 2022, Wiley. (b) Reproduced with permission from ref. 77 Copyright 2022, Wiley.

to 11%, and the thermal stability reached a lifetime of over 400 h for 80% of the initial performance (Fig. 12a). Moreover, brominated polythiophenes hold great application prospects in perovskite solar cells and other emerging optoelectronic devices. In addition, two benchmark conjugated polymers, namely, PM6 and PTB7-Th, were employed in directly synthesized QD devices, which presented favorable energy level alignments. PTB7-Th shows complementary absorption with the synthesized PbS QDs (type II structure). Moreover, the transient absorption and photoluminescence results indicate that the polymer blending strategy can endow fast hole transport from QDs to polymers, enabling the markedly increased photovoltaic performance to 13%. The underlying mechanism can be explained from the “dilution effect” for top-notch photovoltaic polymers with excessively strong aggregation tendency, resulting in moderate feature domain size and surface roughness, which can deliver higher photovoltaic performance (Fig. 12b). This work highlights that aggregation-suppressed polymer blends can offer a facile strategy toward high-performance QD/organic solar cells.

Similarly, for hybrid solar cells with type III bilayer structure, a thin QD film is generally introduced as the front layer for OSCs, which can endow a facile route to address the open

challenge for OSC applications. Kim *et al.* presented a preliminary attempt to build hybrid solar cells with QD front layer and organic bulk heterojunction to enhance their photostability.¹⁷⁶ The results indicated that 13 nm-thick PbS QD layer can meet the need for simultaneous enhancement of PCE and photostability for the PTB7:PC₇₁BM blend. The developed hybrid solar cells exhibited the significantly improved J_{sc} of ~ 17.0 mA cm⁻² over the organic-only counterpart with a J_{sc} of ~ 15.4 mA cm⁻², which mainly stems from the increased light absorption from PbS QDs. Unfortunately, the photostability investigation of hybrid solar cells was missing, which cannot reach the persuasive conclusion that QD film can facilitate the stability improvement of OSCs. Recently, Park *et al.* introduced narrow-gap Indium Arsenide QDs as the main electronic transport layer for OSCs with PM6:Y6 blends, which can deliver a PCE of 15.1%.¹⁷⁷ Moreover, the operating stability of OSCs can be significantly enhanced, retaining over 80% of the initial performance after 1000 min continuous illumination in ambient air, offering strong evidence for the enhanced stability with QD films. More worldwide research efforts are required to perform detailed investigations to address the challenge of OSC stability.

4.2.2 AgBiS₂ QD/organic structure. In terms of the commercial applications, the toxicity of QD materials containing lead and cadmium has significantly compromised their great performance. To counter this issue, environment-friendly QDs, *e.g.*, AgBiS₂ QDs, have witnessed a great advancement in the past few years.^{178–180} Nearly all AgBiS₂ QD solar cells employ promising QD/organic bilayer structures, which generally exhibit great carrier transport. The commonly used organic semiconductor PTB7 can enable high-efficiency carrier extraction, resulting in high FF and J_{sc} , even with an active layer thickness of ~ 30 nm. In 2016, Konstantatos' group developed the first high-performance AgBiS₂ QD solar cells with QD/PTB7 bilayer structures, which can deliver a PCE of 6.3% with only a 35 nm QD layer.⁵⁸ The following research efforts have been devoted to reducing the energy loss of this kind of solar cells from QD synthesis and passivation, which still cannot make further performance breakthrough.^{55,180} For instance, the group further developed a synthetic route to prepare larger-size AgBiS₂ QDs with higher mobility and lower trap density, which present enhanced J_{sc} and reduced energy loss (Fig. 13a–c).⁵⁴ In 2020, Bae *et al.* developed promising AgBiS₂ QD inks with AgI and BiI₃ passivation *via* solution-phase ligand exchange.⁵⁵ The developed solar cells exhibited a record V_{oc} of ~ 0.55 V but a low PCE of $\sim 4.0\%$.

Recently, Konstantatos' group further made a great breakthrough in AgBiS₂ QD solar cells with cation disorder engineering and the promising organic semiconductor PTAA.⁵⁹ They found that cation disorder engineering can lead to the increased absorption, thus enhancing the J_{sc} to ~ 27.0 mA cm⁻². Moreover, they employed the promising PTAA to replace the commonly used PTB7 and further enhance the PCE to over 9%

with a certified efficiency of 8.85% (Fig. 13d–f). The group further developed AgBiS₂ QD inks with 3-mercaptopropionic ligands, which can process with environment-friendly water, resulting in a PCE of 7.3% with a PTAA interface layer.⁵⁶ A recent work by Lee's group revealed that the performance of the AgBiS₂ QD/organic hybrid solar cells can be also enhanced by introducing PM6:BTP-4Cl blend. They employed the commonly used ligands, tetramethylammonium iodide and 2-mercaptoethanol, to provide the great passivation of AgBiS₂ QDs, which could deliver a high PCE of $\sim 9.1\%$ (Fig. 13g–i).⁵⁷ Despite this great advancement, the photovoltaic performance of AgBiS₂ QD solar cells still lagged far behind those of lead chalcogenide QD solar cells (over 15% (ref. 181)) and perovskite QD solar cells (over 17% (ref. 75)). More research efforts are encouraged for further performance breakthrough of such environment-friendly QD solar cells.

4.2.3 Perovskite QD/organic structure. Due to the non-complementarity of absorption and great differences in electrical properties, hybrid perovskite QD/organic solar with bilayer structure mainly employ type I structure. Early reports generally employed the conventional Spiro-OMeTAD as HTLs for perovskite QDSCs and indeed achieved high photovoltaic performance.^{51,52} Nevertheless, the stability issues caused by the complex doping and oxidation processes required by Spiro-OMeTAD have placed great restrictions on their commercial applications.¹⁸² Moreover, the devices with Spiro-OMeTAD generally exhibit the serious hysteresis effect, leading to great PCE difference in forward and reverse scanning directions.^{75,183} Another organic HTL, poly(triarylamine) (PTAA), has been widely used in perovskite solar cells and can enable high photovoltaic performance and stability.^{110,115,184}

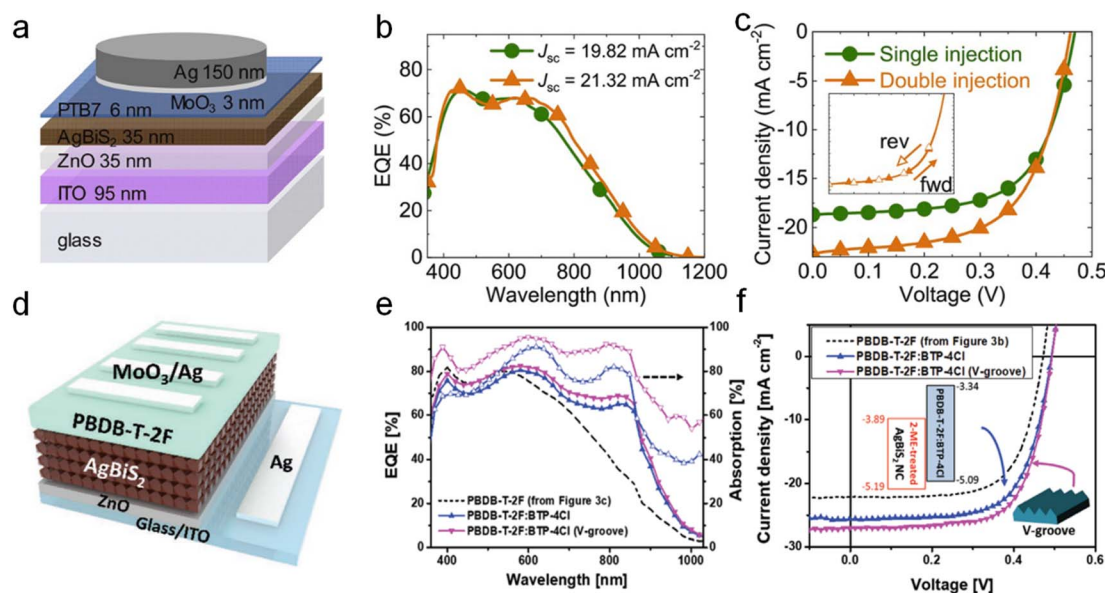


Fig. 13 The device structure and performance of hybrid AgBiS₂ QD/organic solar cells with bilayer structure. (a) Device structure of hybrid solar cell with PTB7 HTL. (b) The EQE of hybrid AgBiS₂ QD/PTB7 solar cells. (c) J - V curves of the hybrid solar cells with PTB7 HTL. (d) Device structure of the hybrid solar cell with PM6 HTL. (e) The EQE of hybrid AgBiS₂ QD/organic solar cells, including PM6 and PM6:BTP-4Cl. (f) J - V curves of the hybrid solar cells with different HTLs. (a–c) Reproduced with permission from ref. 54 Copyright 2020, Elsevier. (d–f) Reproduced with permission from ref. 56 Copyright 2022, Wiley.

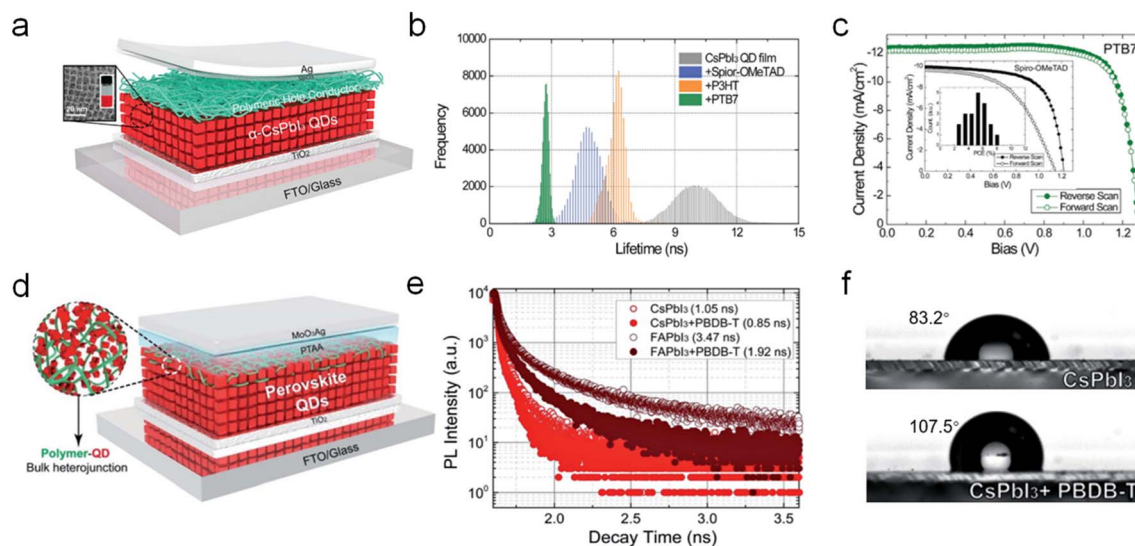


Fig. 14 The device structure and performance of hybrid perovskite QD/organic solar cells with bilayer structure. (a) Device structure of the hybrid solar cell with polymer HTL. (b) Lifetime of QD/polymer heterojunction. (c) J - V curves of the hybrid solar cells with different polymer HTLs. (d) Device structure of the hybrid solar cell with the polymer-QD bulk-heterojunction HTL. (e) Lifetime of the QD/polymer heterojunction with/without introducing the polymer. (f) The contact angles between water droplets and perovskite QDs with/without introducing the polymer. (a–c) Reproduced with permission from ref. 183 Copyright 2018, Elsevier. (e–f) Reproduced with permission from ref. 185 Copyright 2020, The Royal Society of Chemistry.

Except for the commonly used organic HTLs in the perovskite field, organic photovoltaic materials also exhibit great potential for hole extraction. In 2018, Yuan *et al.*¹⁸³ reported that undoped conjugated polymers, *e.g.*, P3HT, PTB7, and PTB7-Th, can achieve a dense and crystalline film under ambient conditions without high-temperature annealing, which is favorable for commercial applications (Fig. 14a). Time-resolved confocal imaging results demonstrated that the perovskite QD/PTB7 structure presented the shortest lifetime, indicating faster carrier extraction (Fig. 14b). With this benefit, the developed hybrid perovskite QD/organic solar cells achieved a high photovoltaic performance with almost no hysteresis (Fig. 14c). In addition, the group further developed a polymer-QD bulk heterojunction hybrid layer coating between the organic HTL and perovskite QD layer, which can improve interfacial charge transfer and reduce carrier recombination loss, resulting in the shorter lifetime and markedly improved photovoltaic performance (Fig. 14d–e).¹⁸⁵ Moreover, the polymer-QD bulk heterojunction exhibited higher moisture resistance with enhanced contact-angle, indicating the change in the QD films from hydrophilicity to hydrophobicity (Fig. 14f).

From the above discussion, we can hold that the type I bilayer structure enabled the significant performance enhancement of hybrid QD:organic solar cells with champion PCEs of 14% and 16.6% for lead chalcogenide and perovskite QDSCs, respectively.^{135,137} Further performance breakthrough requires the improved QD passivation and the matching between QDs and organic HTLs. Crucially, the in-depth understandings of the impact of QD and organic interface on photovoltaic performance may also facilitate the performance and stability of hybrid solar cells. In addition, there exist extremely few reports on type II and type III bilayer structures,

which however can offer a promising route for addressing the challenge of OSC stability. Especially with the increasing OSC performance even up to $\sim 20\%$,¹⁸⁶ the UV instability proves to be the critical limit of their commercial applications. Therefore, hybrid solar cells with QDs and high-efficiency organic blends are expected to contribute to the further success in the photovoltaic field.

4.3 Tandem structure

Tandem structures are one of the ideal building blocks to break through the Shockley–Queisser limit of solar cells and have delivered great success in various solution-processing photovoltaics.^{191,187,188} The unprecedented success of solar cells with tandem structures mainly stems from their superiority that the structure can decouple light absorption and carrier transport, which has been demonstrated to be extremely difficult for single solar cells. Therefore, tandem solar cells can harvest more solar energy without compromising carrier extraction, which can endow the significantly higher photovoltaic performance. Accordingly, tandem OSCs and PSCs have achieved champion PCEs of over 20% and 29.0%, respectively,^{186,189,190} while that for QD-only tandem solar cell lagged behind with a moderate PCE of $\sim 9\%$.^{191,192} Nevertheless, the broad absorption tunability of lead chalcogenide QDs has endowed great potential for tandem structure with organics, which generally cannot harness short-wave solar radiation. Due to the non-complementarity of absorption for perovskite QDs and organic photovoltaic materials, there exist no reports on tandem perovskite QDs and organic solar cells. In this section, we mainly focus on the tandem structure with lead chalcogenide QDs and organics,

and provide a detailed discussion on the recent progress and existing challenges.

For organic and QD tandem solar cells, there exist two general combination routes in terms of light absorption, *i.e.*, with/without complementary absorption for the valley of lead chalcogenide QDs. The superiority of narrow absorption peak of organic photovoltaic materials has laid the foundation for hybrid tandem organic:QD solar cells. Early tandem organic:QD devices generally employed broadband polymer donors and acceptors, which can hardly achieve complementary absorption with the notorious valley of QDs.^{193,194} Integrating QDs with organic bulk heterojunction can mainly broaden the range of solar energy harvesting, which can only slightly improve the photovoltaic performance over single organic and QD subcells. Kim *et al.* employed two blend systems, PBDTTT-C-T:PC₇₁BM and PTB7:PC₇₁BM, as the back-cells, which were tandem with the low-bandgap QD front-cell.¹⁹⁴ After optimizing the intermediate recombination layer (MoO_x/ZnO/PFN), hybrid tandem solar cells can achieve a high V_{oc} of ~ 1.3 V, approaching the sum of the individual subcell voltages. Despite this benefit, the developed tandem solar cells can only deliver a low PCE of $\sim 5\%$, which was even inferior to that of the organic subcell. The poor performance can be mainly attributed to the extremely low J_{sc} of ~ 6 mA cm⁻², which stemmed from the moderate carrier extraction and relatively thin active layer of the subcells. Subsequently, Aqoma *et al.* developed hybrid tandem solar cells with PTB7-Th:PC₇₁BM back-cell and low-band QD front-cell, which presented a slightly higher PCE of $\sim 8.3\%$ compared to the performance of the corresponding OSC-only and QD-only solar cells.¹⁹³ The higher tandem performance can be attributed to the improved J_{sc} of ~ 10.36 mA cm⁻², mainly stemming from partial complementary absorption in the visible band and the optimized intermediate recombination layer (MoO_x/Au/ZnO).

Moreover, the performance of hybrid tandem solar cells can be further improved by modulating the carrier transport of individual subcells. Li *et al.* also employed PTB7-Th:PC₇₁BM back-cell and low-band QD front-cell to develop hybrid tandem solar cells with the introduction of the promising QD HTL into the QD subcell to enhance carrier extraction, thereby resulting in an improved FF of 74.1% and PCE of $\sim 9.12\%$, which is significantly higher than those of the two subcells.¹⁹⁵ From the above discussion, PTB7-Th and fullerene acceptors have been regarded as the model organic blend for hybrid tandem solar cell, which generally employ organic blends as back-cells due to the destruction of QD with the SSLE process on organic subcells. With regard to this issue, Kim *et al.* modified the process of QD deposition and developed a robust intermediate recombination layer (MoO_x/Au/AZO), which jointly enabled the model organic blend as the front-cell.¹⁹⁶ The developed hybrid tandem solar cells presented the improved thickness of the two subcells with 200 nm thick PTB7:PC₆₁BM blend layer and 300 nm PbS QD layer, which yielded a high J_{sc} of ~ 12.6 mA cm⁻² and a state-of-the-art PCE of 9.4%, substantially higher than those of the two subcells. Despite the great progress endowed by the PTB7-Th donor, the missing complementary absorption between the organic blends and QDs still placed great restrictions on the

further progress of hybrid tandem solar cells. Low-bandgap polymers may offer the benefits of complementary absorption for tandem solar cells. Kim *et al.* further introduced low-band PDPP3T with the absorption peak covering the whole absorption valley of PbS QDs into the organic blend with fullerene acceptors.¹⁹⁷ Nevertheless, the developed hybrid tandem solar cells only exhibit a moderate photovoltaic performance of 7.9%, mainly due to the inferior performance of PDPP3T-base subcell with a low J_{sc} .

Owing to the lack of favorable organic blends and imperfect QD passivation, hybrid tandem solar cells encountered a brief stagnation until the development non-fullerene acceptors and high-performance QD inks. Early attempts on low-band polymer for complementary absorption were declared to fail in improving the photovoltaic performance of hybrid tandem solar cells. Some pioneering reports introduced low-band acceptors, *e.g.*, IEICO-4F, for the absorption of QD valley and were successful for hybrid tandem solar cells. Aqoma *et al.* employed the PTB7-Th:IEICO-4F blend as the back-cell and high-performance QD inks for the front-cell, which can offer more facile processing (Fig. 15a).¹⁹⁸ Accordingly, the individual organic and QD solar cells can exhibit PCEs of $\sim 11.0\%$ and 11.2%, respectively, significantly higher than the previous reports. Through transfer-matrix modeling, the champion J_{sc} of ~ 14.0 mA cm⁻² can be achieved with the QD and organic blend of ~ 370 nm and 130 nm, which indicated the great promise of the developed hybrid tandem solar cells (Fig. 15b). With the large-band QD (~ 1.45 eV), the champion photovoltaic performance of $\sim 12.8\%$ was obtained with great complementary absorption with a record J_{sc} of ~ 13.6 mA cm⁻² (Fig. 15c). Further modeling revealed that hybrid solar cells can exhibit promising potential to achieve over 15% PCE by reducing the energy loss of QD subcell and enhancing the light harvesting of organic subcell. Despite the great progress, hybrid tandem solar cells still cannot outperform state-of-the-art QDSCs with the PCE approaching 14%. To bridge the gap, Kim *et al.* developed the hybrid tandem solar cell with PTB7-Th:IEICO-4F blend as the back-cell and PbS QD inks as the front-cell, which can offer significantly higher photovoltaic performance according to the previous report (Fig. 15d).¹⁹⁹ After optimizing the thickness of 90 nm and 450 nm for organic and QD subcells, the modeling champion J_{sc} of ~ 16.0 mA cm⁻² was achieved with the introduction of organic blend HTL for QD subcell (Fig. 15e). Accordingly, the developed hybrid tandem solar cells can deliver a record J_{sc} of ~ 15.2 mA cm⁻² and a champion PCE of $\sim 13.7\%$, which outperformed the most advanced QDSCs for the first time (Fig. 15f).

We proceed to present the existing challenges for the further advancement of hybrid tandem solar cells and the corresponding promising routes to bridge the gap. Compared with organic-only tandem solar cells with a PCE of $\sim 20\%$,¹⁸⁶ hybrid tandem solar cells with organics and lead chalcogenide QDs still lag far behind, mainly due to the large energy loss and the inferior FF. Accordingly, further improving QD passivation may contribute a lot to the reduction of the main energy loss from trap recombination, which is expected to significantly enhance the V_{oc} of hybrid tandem solar cells. In addition, seeking out the

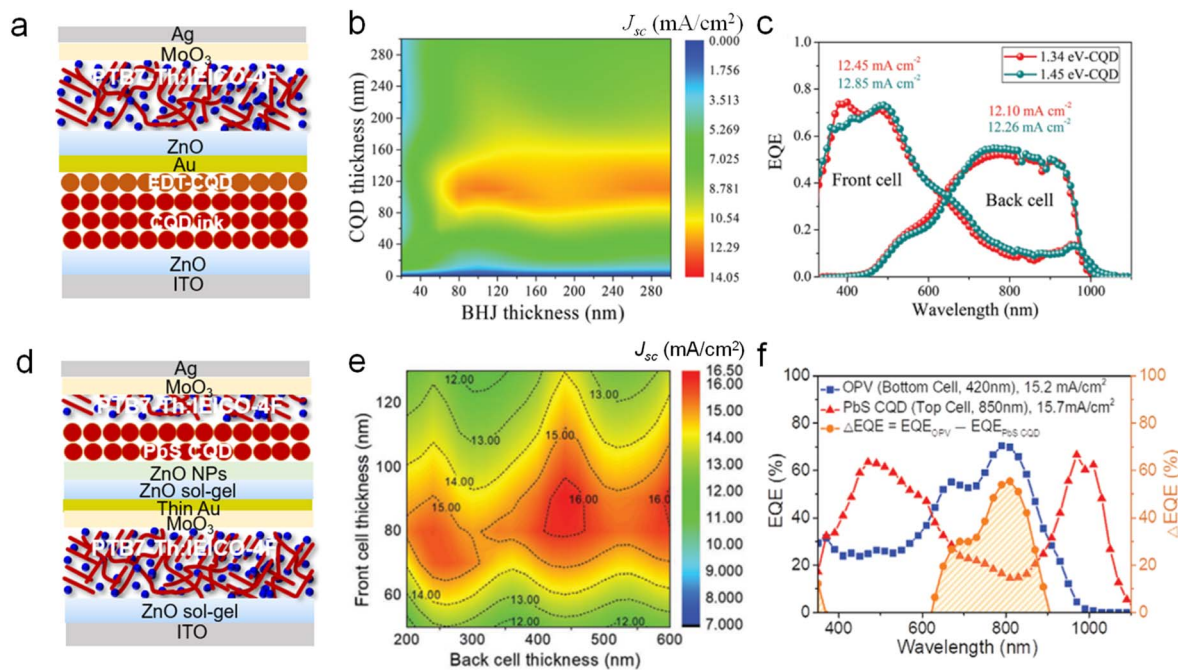


Fig. 15 The device structure and performance of hybrid QD/organic solar cells with tandem structure. (a) and (d) Device structure of hybrid tandem solar cell with QD front cell and organic back cell. (b) and (e) Modeling J_{sc} with the thickness dependence of QD and organic subcells. (c) and (f) EQE spectra of the front and back cells for hybrid tandem solar cells. (a–c) Reproduced with permission from ref. 198 Copyright 2020, Wiley. (d–f) Reproduced with permission from ref. 199 Copyright 2020, Wiley.

favorable polymer donors (PM6 *etc.*) and non-fullerene acceptors (Y6 derivatives) can not only present great complementary absorption but also achieve fast exciton dissociation, which will facilitate the simultaneous improvement of J_{sc} and FF.³⁸ Moreover, unfavorable intermediate recombination layer remains another open challenge, which places great restrictions on further performance improvement of hybrid tandem solar cells. Various ETLs and HTLs from PSCs, OSCs, and QDSCs may offer a promising recombination layer for the tandems. We further provide a summary of the performance of some representative hybrid solar cells (Table 2).

5. Summary and outlook

With regard to the rapid progress of solution-processing solar cells, QDs with broad tunability of bandgap and size-dependent optical and electrical properties can offer the unparalleled benefits for hybrid strategy with organic or perovskite solar cells. Herein, we presented a detailed review covering the recent progress in developing high-performance and high-stability hybrid solar cells with the aim to advance their commercial applications. We firstly discuss in detail the working principles of hybrid QD and organic solar cells, revealing the fundamentals for the combination of QDs and organic photovoltaic materials. Subsequently, we provided an in-depth discussion on QD passivation with organic ligands to further enhance the performance of QDSCs. In addition, hybrid QD and organic solar cells with bulk-heterojunction, bilayer, and tandem structures are systematically summarized to offer some critical

insights for further advancing the commercial applications of hybrid solar cells. Bilayer structures have delivered great success and are expected to further advance the photovoltaic performance of QDSCs and facilitate the large-scale applications. We also highlight the great promise of hybrid solar cells based on bulk-heterojunction and tandem structure, which can offer favorable routes to address the stability issues for OSCs. Despite the rapid progress, there still remain some open challenges for further performance and stability improvement of hybrid solar cells, we proceed to present a brief discussion of the challenges and offer our insights into the corresponding research directions (Fig. 16).

5.1 QD passivation

For lead chalcogenide QDs and AgBiS₂ QDs, there still exists a high defect density, resulting in severe nonradiative recombination and low open-circuit voltage.^{39,100,207} Therefore, it is highly essential to devote more research efforts to developing new passivation strategies to further reduce defect density.^{208–212} Organic ligands have offered great benefits for QD passivation, which were mainly used to develop high-performance QD HTLs. On the other hand, perovskite QDs have witnessed unprecedented progress with the advance of surface passivation. Compared with lead chalcogenide QDs, more and more efforts have centered at developing organic ligands for perfect QD passivation, which can markedly enhance the photovoltaic performance of perovskite QDSCs. Despite the great progress, the performance of perovskite QDSCs still lagged behind their bulk counterparts. Moreover, QD stability in solutions and films

Table 2 The performance of QD and organic hybrid solar cells, including bulk heterojunction, bilayer, and tandem structures

Solar cell structure		V_{oc} (V)	J_{sc} (mA cm ⁻²)	FF (%)	PCE (%)	Ref.	
Bulk-heterojunction	ITO/PDPPTPT:PbS-BDT/LiF/Al	0.47	12.5	49.0	2.9	200	
	ITO/PEDOT:PSS/P3HT:PbS-ArS/LiF/Al	0.56	10.8	50.0	3.0	153	
	ITO/PEDOT:PSS/PSBTBT:PbS _{0.7} Se _{0.3} -EDT/ZnO/Al	0.43	14.9	53.0	3.4	201	
	ITO/PEDOT:PSS/PSBTBT:PbS-EDT/BCP/Mg/Ag	0.63	10.8	51.0	3.4	202	
	ITO/PEDOT:PSS/PDTPBT:PbS-EDT/TiO ₂ /LiF/Al	0.57	13.1	51.0	3.78	155	
	ITO/PEDOT:PSS/PDBT:PbS-BDT/LiF/Al	0.55	13.3	57.0	4.23	156	
	ITO/PEDOT:PSS/Si-PCPDTBT:PbS-PbI ₂ /ZnO/Al	0.48	18.2	55.0	4.78	157	
	ITO/PEDOT:PSS/P3HT:P3HT- <i>b</i> -PS:PbS-BDT/LiF/Al	0.57	16.2	53.2	4.91	154	
	ITO/PEDOT:PSS/PDTPBT:PbS _{0.4} Se _{0.6} -BDT/LiF/Al	0.57	14.7	66.0	5.5	78	
	FTO/TiO ₂ /CsPbI ₃ :Y6/PTAA/MoO ₃ /Ag	1.26	15.8	75.3	15.05	119	
	ITO/SnO ₂ /FAPbI ₃ :ITIC/Spiro-OMeTAD/Ag	1.1	15.4	74.8	12.7	118	
	ITO/SnO ₂ /CsPbI ₃ :PCBM/CsPbI ₃ /PTB7/MoO ₃ /Ag	1.26	15.2	78.0	15.1	158	
	ITO/ZnO ₂ /PTB7-Th:PC ₇₁ BM:CsPbI ₃ /MoO ₃ /Ag	0.81	19.1	65.9	10.84	159	
	ITO/ZnO ₂ /PM6:Y6:CsPbI ₃ /MoO ₃ /Ag	0.84	27.2	72.5	16.6	160	
	Bilayer structure	ITO/ZnO/PbS-BDT/PCPDTTBT/MoO _x /Ag	0.63	13.0	52.0	4.22	203
		ITO/PEDOT:PSS/PDTPBT/PbSe-BDT/LiF/Al	0.58	16.9	49.4	4.83	204
FTO/TiO ₂ /PbS-MPA/P3HT/Au		0.56	18.9	48.2	5.09	163	
FTO/ZnO/PbS-CTAB/BTPA-4/Au		0.44	27.0	46.5	5.55	205	
ITO/PEDOT:PSS/PbS/PTB7:PC ₇₁ BM/Al		0.74	17.0	66.0	8.3	176	
FTO/ZnO/PbS-I/P3HT/Au		0.58	18.4	70.0	7.5	164	
ITO/ZnO/PbS-I QD/PbS-MPA+ p-MeO-TPD/Ag		0.52	28.4	61.8	9.13	43	
ITO/ZnO/PbS-I/PTB7/MoO _x /Ag		0.57	27.9	60.0	9.6	166	
ITO/ZnO/PbS-MPA/α-6T/PEDOT:PSS/Au		0.57	25.6	62.7	9.2	206	
ITO/ZnO/PbS-I/PM6/MoO _x /Ag		0.60	28.4	65.8	11.2	168	
ITO/ZnO/PbS-I QD/PTB7-Th:PC ₇₁ BM/MoO ₃ /Ag		0.65	27.9	66.2	12.0	172	
ITO/ZnO/PbS-I QD/PBDTTPD-HT/MoO ₃ /Ag		0.63	27.4	67.1	11.5	167	
ITO/ZnO/PbS-GuPbI ₃ /PM6/MoO ₃ /Ag		0.62	31.8	65.1	12.8	169	
ITO/ZnO/PbS-I/TIPS-TPD/MoO ₃ /Ag		0.66	28.8	69.0	13.0	170	
ITO/ZnO/PbS-I/PBDTTT-E-T:IEICO/MoO ₃ /Ag		0.66	29.6	67.0	13.1	173	
ITO/ZnO/PbS-I/asy-ranPBTBDT/MoO ₃ /Ag		0.64	29.6	64.1	13.2	171	
ITO/ZnO/PbS-I/PD2FCT-29DPP/MoO ₃ /Ag		0.66	30.3	70.0	14.0	137	
FTO/TiO ₂ /CsPbI ₃ -EtOAc/Spiro-OMeTAD/MoO ₃ /Al		1.23	13.47	65.0	10.77	51	
FTO/TiO ₂ /CsPbI ₃ -FAI/Spiro-OMeTAD/MoO ₃ /Al		1.16	15.25	76.63	13.43	52	
FTO/TiO ₂ /CsPbI ₃ -TPPI/PTAA/MoO ₃ /Ag		1.20	15.2	74.5	13.55	113	
FTO/TiO ₂ /CsPbI ₃ -GASCN/PTAA/MoO ₃ /Ag		1.25	15.85	76.7	15.2	110	
FTO/TiO ₂ /CsPbI ₃ -DPA/PTAA/ MoO ₃ /Ag		1.24	15.84	75.5	14.9	115	
FTO/TiO ₂ /CsPbI ₃ /P3HT/MoO ₃ /Ag	1.23	10.91	73.0	9.82	183		
FTO/TiO ₂ /CsPbI ₃ /PTB7/MoO ₃ /Ag	1.27	12.39	80.0	12.6	183		
FTO/TiO ₂ /CsPbI ₃ /P3HT/MoO ₃ /Ag	1.24	11.05	78.0	10.6	183		
Tandem structure	FTO/TiO ₂ /PbS QD/MoO ₃ /ZnO/PFN PTB7:PC ₆₁ BM/MoO ₃ /Ag	1.25	6.1	69.2	5.3	194	
	ITO/AZO/PbS QD/MoO ₃ /Au/PFN PDPP3T:PC ₆₁ BM/MoO ₃ /Ag	1.25	9.3	67.2	7.9	197	
	ITO/ZnO/PbS QD/MoO ₃ /Au/ZnO PTB7-Th:PC ₇₁ BM/MoO ₃ /Ag	1.27	10.4	63.0	8.3	193	
	ITO/InZnO/PbS-I/PbS-EDT QD/MoO ₃ /Au/ZnO/PTB7-Th:PC ₇₁ BM/MoO ₃ /Ag	1.25	9.9	74.1	9.12	195	
	ITO/ZnO/PTB7:PC ₇₁ BM/MoO ₃ /Au/AZO/PbS QD/MoO ₃ /Au/Ag	1.31	12.5	56.7	9.4	196	
	ITO/ZnO/PbS-I/PbS-EDT QD/Au/ZnO/PTB7-Th:IEICO-4F/MoO ₃ /Ag	1.36	13.6	69.0	12.8	198	
	ITO/ZnO/PTB7-Th:IEICO-4F/MoO ₃ /Au/AZO/PbS QD/PTB7-Th:IEICO-4F/MoO ₃ /Ag	1.34	14.6	68.1	13.3	199	

in ambient conditions should also draw more attention. Therefore, more facile organic ligands are encouraged to be developed for perovskite QDSCs, especially with iodized organic molecules, which can provide additional iodine ions for iodine vacancy of perovskite QDs.

5.2 PbS QD/organic

Recently, hybrid PbS QD/organic solar cells have achieved a great performance breakthrough from ~13% to over 15% with the organic materials (PMMA:PCBM and PMMA-GO) for interface modification.¹⁸¹ This breakthrough revealed the great potential of organic materials for performance advancement of

hybrid solar cells. Hybrid PbS QD/organic solar cells generally employ bulk heterojunctions and bilayer structures. PbS QD/organic bulk heterojunctions can form the favorable energy landscape and complementary absorption, indicating the promising potential for photovoltaic performance improvement. The existing main challenge is the inferior photovoltaic performance, mainly stemming from the essential use of post-treatment for ligand replacing, which will destroy hybrid QD:organic film due to the kinetically hindered process. The emerging co-dissolution strategy may contribute to the further performance improvement. For bilayer structures, type I ones have enabled the significant performance enhancement of

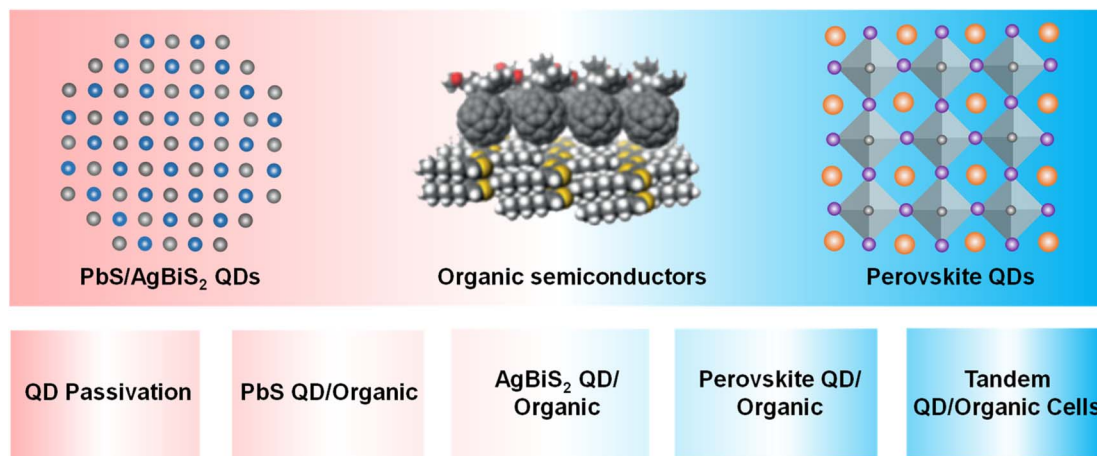


Fig. 16 Summary of the challenges and research directions for the further performance improvement of hybrid solar cells.

hybrid QD/organic solar cells. Further performance breakthrough requires the improved QD passivation and the matching between QDs and organic HTLs. The in-depth understanding of the impact of QD and organic interface on photovoltaic performance may also facilitate the performance and stability of hybrid solar cells. Especially with the increasing OSC performance even up to $\sim 20\%$, the UV instability proves to be a critical limitation of their commercial applications.¹⁸⁶

5.3 AgBiS₂ QD/organic

The European Restriction of Hazardous Substances has limited the use of heavy-metal materials in electronics. The limit of lead element is 1000 ppm by weight of the devices, which has placed great restrictions on the commercial applications of lead chalcogenide QDs and lead-based perovskite QDs. Accordingly, nontoxic QD materials, *e.g.*, AgBiS₂ QDs, exhibit great market competitiveness in the near future. Recently, AgBiS₂ QD solar cells have made a breakthrough in photovoltaic performance from $\sim 6.0\%$ to over 9.0% with great passivation and the matched organic semiconductors.^{56,59} Nevertheless, the performance still lags far behind those of PbS and perovskite QD counterparts, mainly stemming from high energy loss. More efforts should be devoted to improving the passivation of AgBiS₂ QDs and developing favorable organic HTLs. We can draw some inspirations from the promising strategies from PbS QDs.

5.4 Perovskite QD/organic

Hybrid perovskite QD/organic solar cells have witnessed great advances from $\sim 10\%$ to over 16% in the past few years. The top-notch perovskite QD/organic solar cells generally employ bilayer structure and bulk heterojunction for fabricating high-performance devices. The bulk heterojunction can not only provide perfect QD passivation for high-performance QDSCs, but also offer an additional path for the further efficiency breakthrough of OSCs. A better understanding of the morphology modulation for the hybrid QD:organic film is expected to further advance the performance of hybrid solar cells. For bilayer structures, the commonly used organic materials,

spiro-OMeTAD and PTAA still place some restrictions on the further advances of hybrid perovskite QD/organic solar cells. The promising conjugated polymers may hold great potential in further enhancing the performance of hybrid solar cells.^{77,213}

5.5 Tandem QD/organic cells

The broad absorption tunability of QDs has endowed great potential for tandem structure with organic materials,^{214–217} which generally cannot harness short-wave solar radiation. Nevertheless, hybrid tandem solar cells with organics and QDs still lag far behind organic-only tandem solar cells with a PCE of $\sim 20\%$.¹⁸⁶ Accordingly, further improving QD passivation may contribute a lot to the reduction of main energy loss from trap recombination, which is expected to significantly enhance the V_{oc} of hybrid tandem solar cells. In addition, favorable polymer donors and non-fullerene acceptors can offer great complementary absorption and fast exciton dissociation, facilitating both the improvement of J_{sc} and FF.^{218–222} Another open challenge may be the unfavorable intermediate recombination layer, which places great restrictions on further performance enhancement of hybrid tandem solar cells. Various ETLs and HTLs from the emerging solution-processing solar cells may offer promising recombination layers for tandem solar cells.

In brief, QDs with broad tunability of optical and electrical properties can enable unparalleled advantages for the hybrid strategy with OSCs. We believe that the above research directions can enable the further performance and stability improvement of hybrid solar cells and thereby advance the progress toward commercialization.²²³

Conflicts of interest

The authors declare no competing financial interests.

Acknowledgements

The authors would like to especially acknowledge the financial support by the Open Fund of the Hubei Longzhong Laboratory

(No. 2022KF-01). L. Ye also gratefully acknowledges the Peiyang Scholar Program of Tianjin University and the Fundamental Research Funds for the Central Universities. S. Li acknowledges the National Natural Science Foundation of China (No. 51903239). Prof. Z. Zhou would like to acknowledge Tianjin Municipal Science and Technology Bureau of China (Contract No. 21JCZDJC0060). J. Liu would like to acknowledge Shanghai Tongji Gao Tingyao Environmental Protection Technology Development Foundation for support.

References

- J. Jeong, M. Kim, J. Seo, H. Lu, P. Ahlawat, A. Mishra, Y. Yang, M. A. Hope, F. T. Eickemeyer, M. Kim, Y. J. Yoon, I. W. Choi, B. P. Darwich, S. J. Choi, Y. Jo, J. H. Lee, B. Walker, S. M. Zakeeruddin, L. Emsley, U. Rothlisberger, A. Hagfeldt, D. S. Kim, M. Grätzel and J. Y. Kim, *Nature*, 2021, **592**, 381–385.
- J. Peng, D. Walter, Y. Ren, M. Tebyetekerwa, Y. Wu, T. Duong, Q. Lin, J. Li, T. Lu, M. A. Mahmud, O. L. C. Lem, S. Zhao, W. Liu, Y. Liu, H. Shen, L. Li, F. Kremer, H. T. Nguyen, D. Y. Choi, K. J. Weber, K. R. Catchpole and T. P. White, *Science*, 2021, **371**, 390–395.
- M. Jeong, I. W. Choi, E. M. Go, Y. Cho, M. Kim, B. Lee, S. Jeong, Y. Jo, H. W. Choi, J. Lee, J. H. Bae, S. K. Kwak, D. S. Kim and C. Yang, *Science*, 2020, **369**, 1615–1620.
- Y. Wang, M. Ibrahim Dar, L. K. Ono, T. Zhang, M. Kan, Y. Li, L. Zhang, X. Wang, Y. Yang, X. Gao, Y. Qi, M. Grätzel and Y. Zhao, *Science*, 2019, **365**, 591–595.
- Y. Rong, Y. Hu, A. Mei, H. Tan, M. I. Saidaminov, S. Il Seok, M. D. McGehee, E. H. Sargent and H. Han, *Science*, 2018, **361**, 1214.
- I. Massiot, A. Cattoni and S. Collin, *Nat. Energy*, 2020, **5**, 959–972.
- A. Polman, M. Knight, E. C. Garnett, B. Ehrler and W. C. Sinke, *Science*, 2016, **352**, aad4424.
- K. Yoshikawa, H. Kawasaki, W. Yoshida, T. Irie, K. Konishi, K. Nakano, T. Uto, D. Adachi, M. Kanematsu, H. Uzu and K. Yamamoto, *Nat. Energy*, 2017, **2**, 17032.
- S. Essig, C. Allebé, T. Remo, J. F. Geisz, M. A. Steiner, K. Horowitz, L. Barraud, J. S. Ward, M. Schnabel, A. Descoeurdes, D. L. Young, M. Woodhouse, M. Despeisse, C. Ballif and A. Tamboli, *Nat. Energy*, 2017, **2**, 17144.
- Y. Cui, Y. Wang, J. Bergqvist, H. Yao, Y. Xu, B. Gao, C. Yang, S. Zhang, O. Inganäs, F. Gao and J. Hou, *Nat. Energy*, 2019, **4**, 768–775.
- C. Li, J. Zhou, J. Song, J. Xu, H. Zhang, X. Zhang, J. Guo, L. Zhu, D. Wei, G. Han, J. Min, Y. Zhang, Z. Xie, Y. Yi, H. Yan, F. Gao, F. Liu and Y. Sun, *Nat. Energy*, 2021, **6**, 605–613.
- J. Hou, O. Inganäs, R. H. Friend and F. Gao, *Nat. Mater.*, 2018, **17**, 119–128.
- L. Ye, H. Hu, M. Ghasemi, T. Wang, B. A. Collins, J. H. Kim, K. Jiang, J. H. Carpenter, H. Li, Z. Li, T. McAfee, J. Zhao, X. Chen, J. L. Y. Lai, T. Ma, J. L. Bredas, H. Yan and H. Ade, *Nat. Mater.*, 2018, **17**, 253–260.
- L. Meng, Y. Zhang, X. Wan, C. Li, X. Zhang, Y. Wang, X. Ke, Z. Xiao, L. Ding, R. Xia, H. L. Yip, Y. Cao and Y. Chen, *Science*, 2018, **361**, 1094–1098.
- J. H. Choi, H. Wang, S. J. Oh, T. Paik, P. S. Jo, J. Sung, X. Ye, T. Zhao, B. T. Diroll, C. B. Murray and C. R. Kagan, *Science*, 2016, **352**, 205–208.
- F. P. García de Arquer, D. V. Talapin, V. I. Klimov, Y. Arakawa, M. Bayer and E. H. Sargent, *Science*, 2021, **373**, 640.
- J. Xu, O. Voznyy, M. Liu, A. R. Kirmani, G. Walters, R. Munir, M. Abdelsamie, A. H. Proppe, A. Sarkar, F. P. García De Arquer, M. Wei, B. Sun, M. Liu, O. Ouellette, R. Quintero-Bermudez, J. Li, J. Fan, L. Quan, P. Todorovic, H. Tan, S. Hoogland, S. O. Kelley, M. Stefiik, A. Amassian and E. H. Sargent, *Nat. Nanotechnol.*, 2018, **13**, 456–462.
- M. Hao, Y. Bai, S. Zeiske, L. Ren, J. Liu, Y. Yuan, N. Zarrabi, N. Cheng, M. Ghasemi, P. Chen, M. Lyu, D. He, J. H. Yun, Y. Du, Y. Wang, S. Ding, A. Armin, P. Meredith, G. Liu, H. M. Cheng and L. Wang, *Nat. Energy*, 2020, **5**, 79–88.
- M. De Bastiani, A. J. Mirabelli, Y. Hou, F. Gota, E. Aydin, T. G. Allen, J. Troughton, A. S. Subbiah, F. H. Isikgor, J. Liu, L. Xu, B. Chen, E. Van Kerschaver, D. Baran, B. Fraboni, M. F. Salvador, U. W. Paetzold, E. H. Sargent and S. De Wolf, *Nat. Energy*, 2021, **6**, 167–175.
- K. Zhou, K. Xian, Q. Qi, M. Gao, Z. Peng, J. Liu, Y. Liu, S. Li, Y. Zhang, Y. Geng and L. Ye, *Adv. Funct. Mater.*, 2022, **32**, 2201781.
- X. Huang, Y. Cheng, Y. Fang, L. Zhang, X. Hu, S. Y. Jeong, H. Zhang, H. Y. Woo, F. Wu and L. Chen, *Energy Environ. Sci.*, 2022, **15**, 4776–4788.
- J. Liu, M. Gao, J. Kim, Z. Zhou, D. S. Chung, H. Yin and L. Ye, *Mater. Today*, 2021, **51**, 475–503.
- Y. Liu, K. Xian, R. Gui, K. Zhou, J. Liu, M. Gao, W. Zhao, X. Jiao, Y. Deng, H. Yin, Y. Geng and L. Ye, *Macromolecules*, 2022, **55**, 133–145.
- Y. Liu, K. Xian, X. Zhang, M. Gao, Y. Shi, K. Zhou, Y. Deng, J. Hou, Y. Geng and L. Ye, *Macromolecules*, 2022, **55**, 3078–3086.
- S. Karuthedath, J. Gorenflot, Y. Firdaus, N. Chaturvedi, C. S. P. De Castro, G. T. Harrison, J. I. Khan, A. Markina, A. H. Balawi, T. A. Dela Peña, W. Liu, R. Z. Liang, A. Sharma, S. H. K. Paleti, W. Zhang, Y. Lin, E. Alarousu, D. H. Anjum, P. M. Beaujuge, S. De Wolf, I. McCulloch, T. D. Anthopoulos, D. Baran, D. Andrienko and F. Laquai, *Nat. Mater.*, 2021, **20**, 378–384.
- M. Ghasemi, N. Balar, Z. Peng, H. Hu, Y. Qin, T. Kim, J. J. Rech, M. Bidwell, W. Mask, I. McCulloch, W. You, A. Amassian, C. Risko, B. T. O'Connor and H. Ade, *Nat. Mater.*, 2021, **20**, 525–532.
- S. Liu, J. Yuan, W. Deng, M. Luo, Y. Xie, Q. Liang, Y. Zou, Z. He, H. Wu and Y. Cao, *Nat. Photonics*, 2020, **14**, 300–305.
- J. Benduhn, K. Tvingstedt, F. Piersimoni, S. Ullbrich, Y. Fan, M. Tropicano, K. A. McGarry, O. Zeika, M. K. Riede, C. J. Douglas, S. Barlow, S. R. Marder, D. Neher, D. Spoltore and K. Vandewal, *Nat. Energy*, 2017, **2**, 17053.

- 29 X. Che, Y. Li, Y. Qu and S. R. Forrest, *Nat. Energy*, 2018, **3**, 422–427.
- 30 Z. Zheng, H. Yao, L. Ye, Y. Xu, S. Zhang and J. Hou, *Mater. Today*, 2020, **35**, 115–130.
- 31 H. Yin, C. Yan, H. Hu, J. K. W. Ho, X. Zhan, G. Li and S. K. So, *Mater. Sci. Eng., R*, 2020, **140**, 100542.
- 32 L. Zhan, S. Li, Y. Li, R. Sun, J. Min, Z. Bi, W. Ma, Z. Chen, G. Zhou, H. Zhu, M. Shi, L. Zuo and H. Chen, *Joule*, 2022, **6**, 662–675.
- 33 R. Prasanna, T. Leijtens, S. P. Dunfield, J. A. Raiford, E. J. Wolf, S. A. Swifter, J. Werner, G. E. Eperon, C. de Paula, A. F. Palmstrom, C. C. Boyd, M. F. A. M. van Hest, S. F. Bent, G. Teeter, J. J. Berry and M. D. McGehee, *Nat. Energy*, 2019, **4**, 939–947.
- 34 W. Tress, K. Domanski, B. Carlsen, A. Agarwalla, E. A. Alharbi, M. Graetzel and A. Hagfeldt, *Nat. Energy*, 2019, **4**, 568–574.
- 35 Q. Burlingame, M. Ball and Y. L. Loo, *Nat. Energy*, 2020, **5**, 947–949.
- 36 Q. Burlingame, X. Huang, X. Liu, C. Jeong, C. Coburn and S. R. Forrest, *Nature*, 2019, **573**, 394–397.
- 37 P. Bi, S. Zhang, Z. Chen, Y. Xu, Y. Cui, T. Zhang, J. Ren, J. Qin, L. Hong, X. Hao and J. Hou, *Joule*, 2021, **5**, 2408–2419.
- 38 J. Yuan, Y. Zhang, L. Zhou, G. Zhang, H. L. Yip, T. K. Lau, X. Lu, C. Zhu, H. Peng, P. A. Johnson, M. Leclerc, Y. Cao, J. Ulanski, Y. Li and Y. Zou, *Joule*, 2019, **3**, 1140–1151.
- 39 J. Liu, K. Xian, L. Ye and Z. Zhou, *Adv. Mater.*, 2021, **33**, 2008115.
- 40 R. Wang, Y. Shang, P. Kanjanaboos, W. Zhou, Z. Ning and E. H. Sargent, *Energy Environ. Sci.*, 2016, **9**, 1130–1143.
- 41 H. Zhao and F. Rosei, *Chem*, 2017, **3**, 229–258.
- 42 Y. Cao, A. Stavriniadis, T. Lasanta, D. So and G. Konstantatos, *Nat. Energy*, 2016, **1**, 16035.
- 43 S. W. Baek, S. H. Lee, J. H. Song, C. Kim, Y. S. Ha, H. Shin, H. Kim, S. Jeong and J. Y. Lee, *Energy Environ. Sci.*, 2018, **11**, 2078–2084.
- 44 Y. Liu, F. Li, G. Shi, Z. Liu, X. Lin, Y. Shi, Y. Chen, X. Meng, Y. Lv, W. Deng, X. Pan and W. Ma, *ACS Energy Lett.*, 2020, **5**, 3797–3803.
- 45 M. M. Tavakoli, H. T. Dastjerdi, P. Yadav, D. Prochowicz, H. Si and R. Tavakoli, *Adv. Funct. Mater.*, 2021, **31**, 2010623.
- 46 Y. Wang, Z. Liu, N. Huo, F. Li, M. Gu, X. Ling, Y. Zhang, K. Lu, L. Han, H. Fang, A. G. Shulga, Y. Xue, S. Zhou, F. Yang, X. Tang, J. Zheng, M. Antonietta Loi, G. Konstantatos and W. Ma, *Nat. Commun.*, 2019, **10**, 5136.
- 47 A. R. Kirmani, J. M. Luther, M. Abolhasani and A. Amassian, *ACS Energy Lett.*, 2020, **5**, 3069–3100.
- 48 H. Lu, G. M. Carroll, N. R. Neale and M. C. Beard, *ACS Nano*, 2019, **13**, 939–953.
- 49 L. Duan, L. Hu, X. Guan, C. H. Lin, D. Chu, S. Huang, X. Liu, J. Yuan and T. Wu, *Adv. Energy Mater.*, 2021, **11**, 2100354.
- 50 G. W. Guglietta, B. T. Diroll, E. A. Gaulding, J. L. Fordham, S. Li, C. B. Murray and J. B. Baxter, *ACS Nano*, 2015, **9**, 1820–1828.
- 51 A. Swarnkar, A. R. Marshall, E. M. Sanehira, B. D. Chernomordik, D. T. Moore, J. A. Christians, T. Chakrabarti and J. M. Luther, *Science*, 2016, **354**, 92–96.
- 52 E. M. Sanehira, A. R. Marshall, J. A. Christians, S. P. Harvey, P. N. Ciesielski, L. M. Wheeler, P. Schulz, L. Y. Lin, M. C. Beard and J. M. Luther, *Sci. Adv.*, 2017, **3**, eaao4204.
- 53 J. Yuan, A. Hazarika, Q. Zhao, X. Ling, T. Moot, W. Ma and J. M. Luther, *Joule*, 2020, **4**, 1160–1185.
- 54 I. Burgués-Ceballos, Y. Wang, M. Z. Akgul and G. Konstantatos, *Nano Energy*, 2020, **75**, 104961.
- 55 S. Y. Bae, J. T. Oh, J. Y. Park, S. R. Ha, J. Choi, H. Choi and Y. Kim, *Chem. Mater.*, 2020, **32**, 10007–10014.
- 56 C. Kim, I. Kozakci, J. Kim, S. Y. Lee and J. Y. Lee, *Adv. Energy Mater.*, 2022, **12**, 2200262.
- 57 Y. Wang, L. Peng, Z. Wang and G. Konstantatos, *Adv. Energy Mater.*, 2022, **12**, 2200700.
- 58 M. Bernechea, N. C. Miller, G. Xercavins, D. So, A. Stavriniadis and G. Konstantatos, *Nat. Photonics*, 2016, **10**, 521–525.
- 59 Y. Wang, S. R. Kavanagh, I. Burgués-Ceballos, A. Walsh, D. Scanlon and G. Konstantatos, *Nat. Photonics*, 2022, **16**, 235–241.
- 60 H. Zhao, X. Li, M. Cai, C. Liu, Y. You, R. Wang, A. I. Channa, F. Lin, D. Huo, G. Xu, X. Tong and Z. M. Wang, *Adv. Energy Mater.*, 2021, **11**, 2101230.
- 61 Y. You, X. Tong, A. Imran Channa, H. Zhi, M. Cai, H. Zhao, L. Xia, G. Liu, H. Zhao and Z. Wang, *Chem. Eng. J.*, 2022, **452**, 139490.
- 62 Y. You, X. Tong, A. I. Channa, X. Li, C. Liu, H. Ye and Z. Wang, *EcoMat*, 2022, **4**, e12206.
- 63 D. K. Smith, J. M. Luther, O. E. Semonin, A. J. Nozik and M. C. Beard, *ACS Nano*, 2011, **5**, 183–190.
- 64 D. M. Balazs and M. A. Loi, *Adv. Mater.*, 2018, **30**, 1800082.
- 65 G. H. Carey, A. L. Abdelhady, Z. Ning, S. M. Thon, O. M. Bakr and E. H. Sargent, *Chem. Rev.*, 2015, **115**, 12732–12763.
- 66 H. Lee, H. J. Song, M. Shim and C. Lee, *Energy Environ. Sci.*, 2020, **13**, 404–431.
- 67 L. Ye, X. Jiao, M. Zhou, S. Zhang, H. Yao, W. Zhao, A. Xia, H. Ade and J. Hou, *Adv. Mater.*, 2015, **27**, 6046–6054.
- 68 L. Ye, W. Li, X. Guo, M. Zhang and H. Ade, *Chem. Mater.*, 2019, **31**, 6568–6577.
- 69 L. Ye, Y. Xiong, Z. Chen, Q. Zhang, Z. Fei, R. Henry, M. Heeney, B. T. O'Connor, W. You and H. Ade, *Adv. Mater.*, 2019, **31**, 1808153.
- 70 L. Ye, S. Li, X. Liu, S. Zhang, M. Ghasemi, Y. Xiong, J. Hou and H. Ade, *Joule*, 2019, **3**, 443–458.
- 71 K. Lu, Y. Wang, Z. Liu, L. Han, G. Shi, H. Fang, J. Chen, X. Ye, S. Chen, F. Yang, A. G. Shulga, T. Wu, M. Gu, S. Zhou, J. Fan, M. A. Loi and W. Ma, *Adv. Mater.*, 2018, **30**, 1707572.
- 72 Y. Wang, K. Lu, L. Han, Z. Liu, G. Shi, H. Fang, S. Chen, T. Wu, F. Yang, M. Gu, S. Zhou, X. Ling, X. Tang, J. Zheng, M. A. Loi and W. Ma, *Adv. Mater.*, 2018, **30**, 1704871.
- 73 R. Wang, X. Wu, K. Xu, W. Zhou, Y. Shang, H. Tang, H. Chen and Z. Ning, *Adv. Mater.*, 2018, **30**, 1704882.

- 74 Q. A. Akkerman, G. Rainò, M. V. Kovalenko and L. Manna, *Nat. Mater.*, 2018, **17**, 394–405.
- 75 Q. Zhao, A. Hazarika, X. Chen, S. P. Harvey, B. W. Larson, G. R. Teeter, J. Liu, T. Song, C. Xiao, L. Shaw, M. Zhang, G. Li, M. C. Beard and J. M. Luther, *Nat. Commun.*, 2019, **10**, 2842.
- 76 Q. A. Akkerman, M. Gandini, F. Di Stasio, P. Rastogi, F. Palazon, G. Bertoni, J. M. Ball, M. Prato, A. Petrozza and L. Manna, *Nat. Energy*, 2017, **2**, 16194.
- 77 J. Liu, J. Qiao, K. Zhou, J. Wang, R. Gui, K. Xian, M. Gao, H. Yin, X. Hao, Z. Zhou and L. Ye, *Small*, 2022, **18**, 2201387.
- 78 Z. Liu, Y. Sun, J. Yuan, H. Wei, X. Huang, L. Han, W. Wang, H. Wang and W. Ma, *Adv. Mater.*, 2013, **25**, 5772–5778.
- 79 M. S. WDanylo Zherebetsky, Y. Zhang, N. Bronstein, C. Thompson, D. Britt, M. Salmeron, P. Alivisatos and L.-W. Wang, *Science*, 2014, **344**, 1380–1384.
- 80 J. H. Healy, J. D. Bredehoeft, R. L. Wesson, H. Helm, H. Poiraud, A. Etchecopar, R. L. Wesson, W. W. Rubey, N. Lapusta, J. Rice, P. Bernard, A. Kohli, I. Das and M. McClure, *Science*, 2015, **348**, 1226–1229.
- 81 L. M. Wheeler, E. M. Sanehira, A. R. Marshall, P. Schulz, M. Suri, N. C. Anderson, J. A. Christians, D. Nordlund, D. Sokaras, T. Kroll, S. P. Harvey, J. J. Berry, L. Y. Lin and J. M. Luther, *J. Am. Chem. Soc.*, 2018, **140**, 10504–10513.
- 82 J. Park, H. M. Jang, S. Kim, S. H. Jo and T. W. Lee, *Trends Chem.*, 2020, **2**, 837–849.
- 83 F. Cheng, R. He, S. Nie, C. Zhang, J. Yin, J. Li, N. Zheng and B. Wu, *J. Am. Chem. Soc.*, 2021, **143**, 5855–5866.
- 84 M. Yuan, M. Liu and E. H. Sargent, *Nat. Energy*, 2016, **1**, 16016.
- 85 A. G. Pattantyus-Abraham, I. J. Kramer, A. R. Barkhouse, X. Wang, G. Konstantatos, R. Debnath, L. Levina, I. Raabe, M. K. Nazeeruddin, M. Grätzel and E. H. Sargent, *ACS Nano*, 2010, **4**, 3374–3380.
- 86 N. Zhao, T. P. Osedach, L. Y. Chang, S. M. Geyer, D. Wanger, M. T. Binda, A. C. Arango, M. G. Bawendi and V. Bulovic, *ACS Nano*, 2010, **4**, 3743–3752.
- 87 J. Tang, X. Wang, L. Brzozowski, D. A. R. Barkhouse, R. Debnath, L. Levina and E. H. Sargent, *Adv. Mater.*, 2010, **22**, 1398–1402.
- 88 C. Piliago, L. Protesescu, S. Z. Bisri, M. V. Kovalenko and M. A. Loi, *Energy Environ. Sci.*, 2013, **6**, 3054–3059.
- 89 I. J. Kramer, J. C. Minor, G. Moreno-Bautista, L. Rollny, P. Kanjanaboos, D. Kopilovic, S. M. Thon, G. H. Carey, K. W. Chou, D. Zhitomirsky, A. Amassian and E. H. Sargent, *Adv. Mater.*, 2015, **27**, 116–121.
- 90 M. Yuan, O. Voznyy, D. Zhitomirsky, P. Kanjanaboos and E. H. Sargent, *Adv. Mater.*, 2015, **27**, 917–921.
- 91 M. Liu, F. P. G. De Arquer, Y. Li, X. Lan, G. H. Kim, O. Voznyy, L. K. Jagadamma, A. S. Abbas, S. Hoogland, Z. Lu, J. Y. Kim, A. Amassian and E. H. Sargent, *Adv. Mater.*, 2016, **28**, 4142–4148.
- 92 J. Choi, J. W. Jo, F. P. G. de Arquer, Y. B. Zhao, B. Sun, J. Kim, M. J. Choi, S. W. Baek, A. H. Proppe, A. Seifitokaldani, D. H. Nam, P. Li, O. Ouellette, Y. Kim, O. Voznyy, S. Hoogland, S. O. Kelley, Z. H. Lu and E. H. Sargent, *Adv. Mater.*, 2018, **30**, 1801720.
- 93 W. Ahmad, J. He, Z. Liu, K. Xu, Z. Chen, X. Yang, D. Li, Y. Xia, J. Zhang and C. Chen, *Adv. Mater.*, 2019, **31**, 1900593.
- 94 A. R. Kirmani, G. Walters, T. Kim, E. H. Sargent and A. Amassian, *ACS Appl. Energy Mater.*, 2020, **3**, 5385–5392.
- 95 Z. L. Teh, L. Hu, Z. Zhang, A. R. Gentle, Z. Chen, Y. Gao, L. Yuan, Y. Hu, T. Wu, R. J. Patterson and S. Huang, *ACS Appl. Mater. Interfaces*, 2020, **12**, 22751–22759.
- 96 A. Sharma, N. V. Dambhare, J. Bera, S. Sahu and A. K. Rath, *ACS Appl. Nano Mater.*, 2021, **4**, 4016–4025.
- 97 M. Biondi, M. J. Choi, O. Ouellette, S. W. Baek, P. Todorović, B. Sun, S. Lee, M. Wei, P. Li, A. R. Kirmani, L. K. Sagar, L. J. Richter, S. Hoogland, Z. H. Lu, F. P. García de Arquer and E. H. Sargent, *Adv. Mater.*, 2020, **32**, 1906199.
- 98 S. Lee, M. J. Choi, G. Sharma, M. Biondi, B. Chen, S. W. Baek, A. M. Najarian, M. Vafaie, J. Wicks, L. K. Sagar, S. Hoogland, F. P. G. de Arquer, O. Voznyy and E. H. Sargent, *Nat. Commun.*, 2020, **11**, 4814.
- 99 M. J. Choi, F. P. García de Arquer, A. H. Proppe, A. Seifitokaldani, J. Choi, J. Kim, S. W. Baek, M. Liu, B. Sun, M. Biondi, B. Scheffel, G. Walters, D. H. Nam, J. W. Jo, O. Ouellette, O. Voznyy, S. Hoogland, S. O. Kelley, Y. S. Jung and E. H. Sargent, *Nat. Commun.*, 2020, **11**, 103.
- 100 C. H. M. Chuang, A. Maurano, R. E. Brandt, G. W. Hwang, J. Jean, T. Buonassisi, V. Bulović and M. G. Bawendi, *Nano Lett.*, 2015, **15**, 3286–3294.
- 101 S. Pradhan, A. Stavrinadis, S. Gupta, Y. Bi, F. Di Stasio and G. Konstantatos, *Small*, 2017, **13**, 1700598.
- 102 M. Gu, Y. Wang, F. Yang, K. Lu, Y. Xue, T. Wu, H. Fang, S. Zhou, Y. Zhang, X. Ling, Y. Xu, F. Li, J. Yuan, M. A. Loi, Z. Liu and W. Ma, *J. Mater. Chem. A*, 2019, **7**, 15951–15959.
- 103 A. F. Gualdrón-Reyes, S. Masi and I. Mora-Seró, *Trends Chem.*, 2021, **3**, 499–511.
- 104 Y. Bai, M. Hao, S. Ding, P. Chen and L. Wang, *Adv. Mater.*, 2022, **34**, 2105958.
- 105 F. Liu, C. Ding, Y. Zhang, T. Kamisaka, Q. Zhao, J. M. Luther, T. Toyoda, S. Hayase, T. Minemoto, K. Yoshino, B. Zhang, S. Dai, J. Jiang, S. Tao and Q. Shen, *Chem. Mater.*, 2019, **31**, 798–807.
- 106 C. Lu, M. W. Wright, X. Ma, H. Li, D. S. Itanze, J. A. Carter, C. A. Hewitt, G. L. Donati, D. L. Carroll, P. M. Lundin and S. M. Geyer, *Chem. Mater.*, 2019, **31**, 62–67.
- 107 C. Bi, X. Sun, X. Huang, S. Wang, J. Yuan, J. X. Wang, T. Pullerits and J. Tian, *Chem. Mater.*, 2020, **32**, 6105–6113.
- 108 L. Zhang, C. Kang, G. Zhang, Z. Pan, Z. Huang, S. Xu, H. Rao, H. Liu, S. Wu, X. Wu, X. Li, Z. Zhu, X. Zhong and A. K. Y. Jen, *Adv. Funct. Mater.*, 2020, **31**, 2005930.
- 109 K. Chen, Q. Zhong, W. Chen, B. Sang, Y. Wang, T. Yang, Y. Liu, Y. Zhang and H. Zhang, *Adv. Funct. Mater.*, 2019, **29**, 1900991.
- 110 X. Ling, J. Yuan, X. Zhang, Y. Qian, S. M. Zakeeruddin, B. W. Larson, Q. Zhao, J. Shi, J. Yang, K. Ji, Y. Zhang, Y. Wang, C. Zhang, S. Duhm, J. M. Luther, M. Grätzel and W. Ma, *Adv. Mater.*, 2020, **32**, 2001906.
- 111 J. Shi, F. Li, Y. Jin, C. Liu, B. Cohen-Kleinstejn, S. Yuan, Y. Li, Z. K. Wang, J. Yuan and W. Ma, *Angew. Chem., Int. Ed.*, 2020, **59**, 22230–22237.

- 112 D. Jia, J. Chen, X. Mei, W. Fan, S. Luo, M. Yu, J. Liu and X. Zhang, *Energy Environ. Sci.*, 2021, **14**, 4599–4609.
- 113 Y. Wang, C. Duan, X. Zhang, J. Sun, X. Ling, J. Shi, L. Hu, Z. Zhou, X. Wu, W. Han, X. Liu, C. Cazorla, D. Chu, S. Huang, T. Wu, J. Yuan and W. Ma, *Adv. Funct. Mater.*, 2021, **32**, 2108615.
- 114 J. Kim, S. Cho, F. Dinic, J. Choi, C. Choi, S. M. Jeong, J. S. Lee, O. Voznyy, M. J. Ko and Y. Kim, *Nano Energy*, 2020, **75**, 104985.
- 115 Y. Wang, J. Yuan, X. Zhang, X. Ling, B. W. Larson, Q. Zhao, Y. Yang, Y. Shi, J. M. Luther and W. Ma, *Adv. Mater.*, 2020, **32**, 2000449.
- 116 J. Chen, D. Jia, J. Qiu, R. Zhuang, Y. Hua and X. Zhang, *Nano Energy*, 2022, **96**, 107140.
- 117 D. Jia, J. Chen, M. Yu, J. Liu, E. M. J. Johansson, A. Hagfeldt and X. Zhang, *Small*, 2020, **16**, 2001772.
- 118 J. Xue, R. Wang, L. Chen, S. Nuryyeva, T. H. Han, T. Huang, S. Tan, J. Zhu, M. Wang, Z. K. Wang, C. Zhang, J. W. Lee and Y. Yang, *Adv. Mater.*, 2019, **31**, 1900111.
- 119 J. Yuan, X. Zhang, J. Sun, R. Patterson, H. Yao, D. Xue, Y. Wang, K. Ji, L. Hu, S. Huang, D. Chu, T. Wu, J. Hou and J. Yuan, *Adv. Funct. Mater.*, 2021, **31**, 2101272.
- 120 J. A. Dias, S. H. Santagneli, S. J. L. Ribeiro and Y. Messaddeq, *Sol. RRL*, 2021, **5**, 2100205.
- 121 J. Chen, D. Jia, E. M. J. Johansson, A. Hagfeldt and X. Zhang, *Energy Environ. Sci.*, 2021, **14**, 224–261.
- 122 X. Ling, S. Zhou, J. Yuan, J. Shi, Y. Qian, B. W. Larson, Q. Zhao, C. Qin, F. Li, G. Shi, C. Stewart, J. Hu, X. Zhang, J. M. Luther, S. Duham and W. Ma, *Adv. Energy Mater.*, 2019, **9**, 1900721.
- 123 J. Yuan, C. Bi, S. Wang, R. Guo, T. Shen, L. Zhang and J. Tian, *Adv. Funct. Mater.*, 2019, **29**, 1906615.
- 124 W. Yang, R. Su, D. Luo, Q. Hu, F. Zhang, Z. Xu, Z. Wang, J. Tang, Z. Lv, X. Yang, Y. Tu, W. Zhang, H. Zhong, Q. Gong, T. P. Russell and R. Zhu, *Nano Energy*, 2020, **67**, 104189.
- 125 X. Zhang, H. Huang, Y. M. Maung, J. Yuan and W. Ma, *Chem. Commun.*, 2021, **57**, 7906–7909.
- 126 J. M. Luther, J. Gao, M. T. Lloyd, O. E. Semonin, M. C. Beard and A. J. Nozik, *Adv. Mater.*, 2010, **22**, 3704–3707.
- 127 A. H. Ip, A. Kiani, I. J. Kramer, O. Voznyy, H. F. Movahed, L. Levina, M. M. Adachi, S. Hoogland and E. H. Sargent, *ACS Nano*, 2015, **9**, 8833–8842.
- 128 H. Aqoma and S. Y. Jang, *Energy Environ. Sci.*, 2018, **11**, 1603–1609.
- 129 J. Khan, X. Zhang, J. Yuan, Y. Wang, G. Shi, R. Patterson, J. Shi, X. Ling, L. Hu, T. Wu, S. Dai and W. Ma, *ACS Energy Lett.*, 2020, **5**, 3322–3329.
- 130 D. Jia, J. Chen, X. Mei, W. Fan, S. Luo, M. Yu, J. Liu and X. Zhang, *Energy Environ. Sci.*, 2021, **14**, 4599–4609.
- 131 J. Kim, B. Koo, W. H. Kim, J. Choi, C. Choi, S. J. Lim, J. S. Lee, D. H. Kim, M. J. Ko and Y. Kim, *Nano Energy*, 2019, **66**, 104130.
- 132 H. Wei, H. Zhang, H. Sun and B. Yang, *Nano Today*, 2012, **7**, 316–326.
- 133 M. J. Greaney and R. L. Brutchey, *Mater. Today*, 2015, **18**, 31–38.
- 134 Z. Chen, X. Du, Q. Zeng and B. Yang, *Mater. Chem. Front.*, 2017, **1**, 1502–1513.
- 135 M. Hao, Y. Bai, S. Zeiske, L. Ren, J. Liu, Y. Yuan, N. Zarrabi, N. Cheng, M. Ghasemi, P. Chen, M. Lyu, D. He, J. H. Yun, Y. Du, Y. Wang, S. Ding, A. Armin, P. Meredith, G. Liu, H. M. Cheng and L. Wang, *Nat. Energy*, 2020, **5**, 79–88.
- 136 B. Sun, A. Johnston, C. Xu, M. Wei, Z. Huang, Z. Jiang, H. Zhou, Y. Gao, Y. Dong, O. Ouellette, X. Zheng, J. Liu, M. J. Choi, Y. Gao, S. W. Baek, F. Laquai, O. M. Bakr, D. Ban, O. Voznyy, F. P. García de Arquer and E. H. Sargent, *Joule*, 2020, **4**, 1542–1556.
- 137 H. Il Kim, S. W. Baek, H. J. Cheon, S. U. Ryu, S. Lee, M. J. Choi, K. Choi, M. Biondi, S. Hoogland, F. P. G. de Arquer, S. K. Kwon, Y. H. Kim, T. Park and E. H. Sargent, *Adv. Mater.*, 2020, **32**, 2004985.
- 138 S. W. Tsang, H. Fu, R. Wang, J. Lu, K. Yu and Y. Tao, *Appl. Phys. Lett.*, 2009, **95**, 183505.
- 139 K. M. Noone, N. C. Anderson, N. E. Horwitz, A. M. Munro, A. P. Kulkarni and D. S. Ginger, *ACS Nano*, 2009, **3**, 1345–1352.
- 140 Y. Zhang and Z. Xu, *Appl. Phys. Lett.*, 2008, **93**, 2006–2009.
- 141 D. Cui, J. Xu, T. Zhu, G. Paradee, S. Ashok and M. Gerhold, *Appl. Phys. Lett.*, 2006, **88**, 2004–2007.
- 142 S. A. McDonald, G. Konstantatos, S. Zhang, P. W. Cyr, E. J. D. Klem, L. Levina and E. H. Sargent, *Nat. Mater.*, 2005, **4**, 138–142.
- 143 A. Gocalińska, M. Saba, F. Quochi, M. Marceddu, K. Szendrei, J. Gao, M. A. Loi, M. Yarema, R. Seyrkammer, W. Heiss, A. Mura and G. Bongiovanni, *J. Phys. Chem. Lett.*, 2010, **1**, 1149–1154.
- 144 A. Guchhait, A. K. Rath and A. J. Pal, *Appl. Phys. Lett.*, 2010, **96**, 073505.
- 145 J. Seo, S. J. Kim, W. J. Kim, R. Singh, M. Samoc, A. N. Cartwright and P. N. Prasad, *Nanotechnology*, 2009, **20**, 095202.
- 146 E. Strein, A. Colbert, S. Subramaniyan, H. Nagaoka, C. W. Schlenker, E. Janke, S. A. Jenekhe and D. S. Ginger, *Energy Environ. Sci.*, 2013, **6**, 769–775.
- 147 Y. Firdaus, R. Miranti, E. Fron, A. Khetubol, E. Vandenplas, D. Cheyns, H. Borchert, J. Parisi and M. Van Der Auweraer, *J. Appl. Phys.*, 2015, **118**, 055502.
- 148 Y. Firdaus, E. Vandenplas, A. Khetubol, D. Cheyns, R. Gehlhaar and M. Van Der Auweraer, *J. Appl. Phys.*, 2015, **117**, 095503.
- 149 V. Bertasius, R. Mastria, A. Rizzo, G. Gigli, C. Giansante and V. Gulbinas, *J. Phys. Chem. C*, 2016, **120**, 14356–14364.
- 150 W. Guo, J. Yuan, H. Yuan, F. Jin, L. Han, C. Sheng, W. Ma and H. Zhao, *Adv. Funct. Mater.*, 2016, **26**, 713–721.
- 151 Y. Firdaus, E. Vandenplas, Y. Justo, R. Gehlhaar, D. Cheyns, Z. Hens and M. Van Der Auweraer, *J. Appl. Phys.*, 2014, **116**, 094305.
- 152 F. Alam, N. Kumar and V. Dutta, *Org. Electron.*, 2015, **22**, 44–50.
- 153 C. Giansante, R. Mastria, G. Lerario, L. Moretti, I. Kriegel, F. Scotognella, G. Lanzani, S. Carallo, M. Esposito, M. Biasiucci, A. Rizzo and G. Gigli, *Adv. Funct. Mater.*, 2015, **25**, 111–119.

- 154 D.-T. Nguyen, S. Sharma, S.-A. Chen, P. V. Komarov, V. A. Ivanov and A. R. Khokhlov, *Mater. Adv.*, 2021, **2**, 1016–1023.
- 155 J. Seo, M. J. Cho, D. Lee, A. N. Cartwright and P. N. Prasad, *Adv. Mater.*, 2011, **23**, 3984–3988.
- 156 J. Yuan, A. Gallagher, Z. Liu, Y. Sun and W. Ma, *J. Mater. Chem. A*, 2015, **3**, 2572–2579.
- 157 H. Lu, J. Joy, R. L. Gaspar, S. E. Bradforth and R. L. Brutchey, *Chem. Mater.*, 2016, **28**, 1897–1906.
- 158 L. Hu, Q. Zhao, S. Huang, J. Zheng, X. Guan, R. Patterson, J. Kim, L. Shi, C. H. Lin, Q. Lei, D. Chu, W. Tao, S. Cheong, R. D. Tilley, A. W. Y. Ho-Baillie, J. M. Luther, J. Yuan and T. Wu, *Nat. Commun.*, 2021, **12**, 466.
- 159 N. Guijarro, L. Yao, F. Le Formal, R. A. Wells, Y. Liu, B. P. Darwich, L. Navratilova, H. H. Cho, J. H. Yum and K. Sivula, *Angew. Chem., Int. Ed.*, 2019, **58**, 12696–12704.
- 160 Y. Wang, B. Jia, J. Wang, P. Xue, Y. Xiao, T. Li, J. Wang, H. Lu, Z. Tang, X. Lu, F. Huang and X. Zhan, *Adv. Mater.*, 2020, **32**, 2002066.
- 161 J. Kim, O. Ouellette, O. Voznyy, M. Wei, J. Choi, M. J. Choi, J. W. Jo, S. W. Baek, J. Fan, M. I. Saidaminov, B. Sun, P. Li, D. H. Nam, S. Hoogland, Z. H. Lu, F. P. García de Arquer and E. H. Sargent, *Adv. Mater.*, 2018, **30**, 1803830.
- 162 L. Ye, B. A. Collins, X. Jiao, J. Zhao, H. Yan and H. Ade, *Adv. Energy Mater.*, 2018, **8**, 1703058.
- 163 X. Zhang, Y. Justo, J. Maes, W. Walravens, J. Zhang, J. Liu, Z. Hens and E. M. J. Johansson, *J. Mater. Chem. A*, 2015, **3**, 20579–20585.
- 164 D. C. J. Neo, N. Zhang, Y. Tazawa, H. Jiang, G. M. Hughes, C. R. M. Grovenor, H. E. Assender and A. A. R. Watt, *ACS Appl. Mater. Interfaces*, 2016, **8**, 12101–12108.
- 165 J. Wang, J. Liu, K. Zhou, K. Xian, Q. Qi, W. Zhao, Y. Chen and L. Ye, *Sol. RRL*, 2022, **6**, 2200779.
- 166 H. Aqoma, M. Al Mubarak, W. Lee, W. T. Hadmojo, C. Park, T. K. Ahn, D. Y. Ryu and S. Y. Jang, *Adv. Energy Mater.*, 2018, **8**, 1800572.
- 167 M. Al Mubarak, H. Aqoma, F. T. A. Wibowo, W. Lee, H. M. Kim, D. Y. Ryu, J. W. Jeon and S. Y. Jang, *Adv. Energy Mater.*, 2020, **10**, 1902933.
- 168 Y. Xue, F. Yang, J. Yuan, Y. Zhang, M. Gu, Y. Xu, X. Ling, Y. Wang, F. Li, T. Zhai, J. Li, C. Cui, Y. Chen and W. Ma, *ACS Energy Lett.*, 2019, **4**, 2850–2858.
- 169 J. Yang, S. C. Cho, S. Lee, J. W. Yoon, W. H. Jeong, H. Song, J. T. Oh, S. G. Lim, S. Y. Bae, B. R. Lee, M. Ahmadi, E. H. Sargent, W. Yi, S. U. Lee and H. Choi, *ACS Nano*, 2022, **16**, 1649–1660.
- 170 M. Al Mubarak, F. T. A. Wibowo, H. Aqoma, N. Vamsi Krishna, W. Lee, D. Y. Ryu, S. Cho, I. H. Jung and S. Y. Jang, *ACS Energy Lett.*, 2020, **5**, 3452–3460.
- 171 H. Il Kim, J. Lee, M. J. Choi, S. U. Ryu, K. Choi, S. Lee, S. Hoogland, F. P. G. de Arquer, E. H. Sargent and T. Park, *Adv. Energy Mater.*, 2020, **10**, 2002084.
- 172 Y. Zhang, Y. Kan, K. Gao, M. Gu, Y. Shi, X. Zhang, Y. Xue, X. Zhang, Z. Liu, Y. Zhang, J. Yuan, W. Ma and A. K. Y. Jen, *ACS Energy Lett.*, 2020, **5**, 2335–2342.
- 173 S. W. Baek, S. Jun, B. Kim, A. H. Proppe, O. Ouellette, O. Voznyy, C. Kim, J. Kim, G. Walters, J. H. Song, S. Jeong, H. R. Byun, M. S. Jeong, S. Hoogland, F. P. García de Arquer, S. O. Kelley, J. Y. Lee and E. H. Sargent, *Nat. Energy*, 2019, **4**, 969–976.
- 174 J. Liu, J. Wang, K. Xian, W. Zhao, Z. Zhou, S. Li and L. Ye, *Chem. Commun.*, 2023, DOI: [10.1039/d2cc05281d](https://doi.org/10.1039/d2cc05281d).
- 175 J. Liu, Y. Liu, J. Wang, H. Li, K. Zhou, R. Gui, K. Xian, Q. Qi, X. Yang, Y. Chen, W. Zhao and H. Yin, Kui Zhao, Zhihua Zhou and Long Ye, *Adv. Energy Mater.*, 2022, **12**, 2201975.
- 176 G. H. Kim, B. Walker, D. Zhitomirsky, J. Heo, S. J. Ko, J. Park, E. H. Sargent and J. Young Kim, *Nano Energy*, 2015, **13**, 491–499.
- 177 Y. Park, S. Y. Bae, T. Kim, S. Park, J. T. Oh, D. Shin, M. Choi, H. Kim, B. Kim, D. C. Lee, J. H. Song, H. Choi, S. Jeong and Y. Kim, *Adv. Energy Mater.*, 2022, **12**, 2104018.
- 178 D. Becker-Koch, M. Albaladejo-Siguan, Y. J. Hofstetter, O. Solomeshch, D. Pohl, B. Rellinghaus, N. Tessler and Y. Vaynzof, *ACS Appl. Mater. Interfaces*, 2021, **13**, 18750–18757.
- 179 M. Z. Akgul and G. Konstantatos, *ACS Appl. Nano Mater.*, 2021, **4**, 2887–2894.
- 180 L. Hu, R. J. Patterson, Z. Zhang, Y. Hu, D. Li, Z. Chen, L. Yuan, Z. L. Teh, Y. Gao, G. J. Conibeer and S. Huang, *J. Mater. Chem. C*, 2018, **6**, 731–737.
- 181 C. Ding, D. Wang, L. Dong, H. Li and Y. Li, *Adv. Energy Mater.*, 2022, **12**, 2201676.
- 182 K. Chen, W. Jin, Y. Zhang, T. Yang, P. Reiss, Q. Zhong, U. Bach, Q. Li, Y. Wang, H. Zhang, Q. Bao and Y. Liu, *J. Am. Chem. Soc.*, 2020, **142**, 3775–3783.
- 183 J. Yuan, X. Ling, D. Yang, F. Li, S. Zhou, J. Shi, Y. Qian, J. Hu, Y. Sun, Y. Yang, X. Gao, S. Duhm, Q. Zhang and W. Ma, *Joule*, 2018, **2**, 2450–2463.
- 184 X. Zhang, H. Huang, X. Ling, J. Sun, X. Jiang, Y. Wang, D. Xue, L. Huang, L. Chi, J. Yuan and W. Ma, *Adv. Mater.*, 2022, **34**, 2105977.
- 185 K. Ji, J. Yuan, F. Li, Y. Shi, X. Ling, X. Zhang, Y. Zhang, H. Lu, J. Yuan and W. Ma, *J. Mater. Chem. A*, 2020, **8**, 8104–8112.
- 186 Z. Zheng, J. Wang, P. Bi, J. Ren, Y. Wang, Y. Yang, X. Liu, S. Zhang and J. Hou, *Joule*, 2022, **6**, 171–184.
- 187 D. Kim, H. J. Jung, I. J. Park, B. W. Larson, S. P. Dunfield, C. Xiao, J. Kim, J. Tong, P. Boonmongkolras, S. G. Ji, F. Zhang, S. R. Pae, M. Kim, S. B. Kang, V. Dravid, J. J. Berry, J. Y. Kim, K. Zhu, D. H. Kim and B. Shin, *Science*, 2020, **368**, 155–160.
- 188 D. N. Weiss, *Joule*, 2021, **5**, 2247–2250.
- 189 J. Liu, E. Aydin, J. Yin, M. De Bastiani, F. H. Isikgor, A. U. Rehman, E. Yengel, E. Ugur, G. T. Harrison, M. Wang, Y. Gao, J. I. Khan, M. Babics, T. G. Allen, A. S. Subbiah, K. Zhu, X. Zheng, W. Yan, F. Xu, M. F. Salvador, O. M. Bakr, T. D. Anthopoulos, M. Lanza, O. F. Mohammed, F. Laquai and S. De Wolf, *Joule*, 2021, **5**, 3169–3186.
- 190 A. Al-Ashouri, E. Köhnen, B. Li, A. Magomedov, H. Hempel, P. Caprioglio, J. A. Márquez, A. B. M. Vilches, E. Kasparavicius, J. A. Smith, N. Phung, D. Menzel, M. Grischek, L. Kegelmann, D. Skroblin, C. Gollwitzer, T. Malinauskas, M. Jošt, G. Matič, B. Rech,

- R. Schlatmann, M. Topič, L. Korte, A. Abate, B. Stannowski, D. Neher, M. Stolterfoht, T. Unold, V. Getautis and S. Albrecht, *Science*, 2020, **370**, 1300–1309.
- 191 G. Shi, Y. Wang, Z. Liu, L. Han, J. Liu, Y. Wang, K. Lu, S. Chen, X. Ling, Y. Li, S. Cheng and W. Ma, *Adv. Energy Mater.*, 2017, **7**, 1602667.
- 192 Y. Bi, S. Pradhan, M. Z. Akgul, S. Gupta, A. Stavrinadis, J. Wang and G. Konstantatos, *ACS Energy Lett.*, 2018, **3**, 1753–1759.
- 193 H. Aqoma, R. Azmi, S. H. Oh and S. Y. Jang, *Nano Energy*, 2017, **31**, 403–409.
- 194 T. Kim, Y. Gao, H. Hu, B. Yan, Z. Ning, L. K. Jagadamma, K. Zhao, A. R. Kirmani, J. Eid, M. M. Adachi, E. H. Sargent, P. M. Beaujuge and A. Amassian, *Nano Energy*, 2015, **17**, 196–205.
- 195 Y. Li, P. Yeh, S. Sharma and S. Chen, *J. Mater. Chem. A*, 2017, **5**, 21528–21535.
- 196 T. Kim, Y. Firdaus, A. R. Kirmani, R. Z. Liang, H. Hu, M. Liu, A. El Labban, S. Hoogland, P. M. Beaujuge, E. H. Sargent and A. Amassian, *ACS Energy Lett.*, 2018, **3**, 1307–1314.
- 197 A. R. Kirmani, Y. Firdaus, Y. Gao, A. Sheikh, M. Yuan, O. F. Mohammed, S. Hoogland, P. M. Beaujuge and E. H. Sargent, *Appl. Phys. Lett.*, 2017, **110**, 223903.
- 198 H. Aqoma, I. F. Imran, M. Al Mubarak, W. T. Hadmojo, Y. R. Do and S. Y. Jang, *Adv. Energy Mater.*, 2020, **10**, 1903294.
- 199 H. Il Kim, S. W. Baek, M. J. Choi, B. Chen, O. Ouellette, K. Choi, B. Scheffel, H. Choi, M. Biondi, S. Hoogland, F. P. García de Arquer, T. Park and E. H. Sargent, *Adv. Mater.*, 2020, **32**, 2004657.
- 200 C. Piliago, M. Manca, R. Kroon, M. Yarema, K. Szendrei, M. R. Andersson, W. Heiss and M. A. Loi, *J. Mater. Chem.*, 2012, **22**, 24411–24416.
- 201 M. Nam, S. Kim, S. Kim, S. W. Kim and K. Lee, *Nanoscale*, 2013, **5**, 8202–8209.
- 202 M. Nam, J. Park, S. W. Kim and K. Lee, *J. Mater. Chem. A*, 2014, **2**, 3978–3985.
- 203 Y. Zhang, Z. Li, J. Ouyang, S. W. Tsang, J. Lu, K. Yu, J. Ding and Y. Tao, *Org. Electron.*, 2012, **13**, 2773–2780.
- 204 Y. Sun, Z. Liu, J. Yuan, J. Chen, Y. Zhou, X. Huang and W. Ma, *Org. Electron.*, 2015, **24**, 263–271.
- 205 Y. Zhang, G. Wu, I. Mora-Seró, C. Ding, F. Liu, Q. Huang, Y. Ogomi, S. Hayase, T. Toyoda, R. Wang, J. Otsuki and Q. Shen, *J. Phys. Chem. Lett.*, 2017, **8**, 2163–2169.
- 206 H. Lim, D. Kim, M. J. Choi, E. H. Sargent, Y. S. Jung and J. Y. Kim, *Adv. Energy Mater.*, 2019, **9**, 1901938.
- 207 R. H. Gilmore, Y. Liu, W. Shcherbakov-Wu, N. S. Dahod, E. M. Y. Lee, M. C. Weidman, H. Li, J. Jean, V. Bulović, A. P. Willard, J. C. Grossman and W. A. Tisdale, *Matter*, 2019, **1**, 250–265.
- 208 C. Ding, F. Liu, Y. Zhang, S. Hayase, T. Masuda, R. Wang, Y. Zhou, Y. Yao, Z. Zou and Q. Shen, *ACS Energy Lett.*, 2020, **5**, 3224–3236.
- 209 Y. Liu, D. Kim, O. P. Morris, D. Zhitomirsky and J. C. Grossman, *ACS Nano*, 2018, **12**, 2838–2845.
- 210 M. Biondi, M. J. Choi, Z. Wang, M. Wei, S. Lee, H. Choubisa, L. K. Sagar, B. Sun, S. W. Baek, B. Chen, P. Todorović, A. M. Najarian, A. Sedighian Rasouli, D. H. Nam, M. Vafaie, Y. C. Li, K. Bertens, S. Hoogland, O. Voznyy, F. P. García de Arquer and E. H. Sargent, *Adv. Mater.*, 2021, **33**, 2101056.
- 211 J. Choi, M. J. Choi, J. Kim, F. Dinic, P. Todorovic, B. Sun, M. Wei, S. W. Baek, S. Hoogland, F. P. García de Arquer, O. Voznyy and E. H. Sargent, *Adv. Mater.*, 2020, **32**, 1906497.
- 212 Y. Lin, T. Gao, X. Pan, M. Kamenetska and S. M. Thon, *Adv. Mater.*, 2020, **32**, 1906602.
- 213 Q. Fu, X. Tang, H. Liu, R. Wang, T. Liu, Z. Wu, H. Y. Woo, T. Zhou, X. Wan, Y. Chen and Y. Liu, *J. Am. Chem. Soc.*, 2022, **144**, 9500–9509.
- 214 G. X. Jia, S. Q. Zhang, L. Yang, C. He, H. L. Fan and J. H. Hou, *Acta Phys.-Chim. Sin.*, 2019, **35**, 76–83.
- 215 Y. Chen, H. Chen, H. Guan, W. Liu, Z. Li, H. Liu, Y. Li and Y. Zou, *Chin. Chem. Lett.*, 2021, **32**, 229–233.
- 216 N. Wang, W. Yang, S. Li, M. Shi, T. K. Lau, X. Lu, R. Shikler, C. Z. Li and H. Chen, *Chin. Chem. Lett.*, 2019, **30**, 1277–1281.
- 217 M. Gao, Y. Liu, K. Xian, Z. Peng, K. Zhou, J. Liu, S. Li, F. Xie, W. Zhao, J. Zhang, X. Jiao and L. Ye, *Aggregate*, 2022, e190.
- 218 A. Karki, J. Vollbrecht, A. J. Gillett, S. S. Xiao, Y. Yang, Z. Peng, N. Schopp, A. L. Dixon, S. Yoon, M. Schrock, H. Ade, G. N. M. Reddy, R. H. Friend and T. Q. Nguyen, *Energy Environ. Sci.*, 2020, **13**, 3679–3692.
- 219 C. Yang, S. Zhang, J. Ren, M. Gao, P. Bi, J. Hou, S. Zhang, L. Ye and J. Hou, *Energy Environ. Sci.*, 2020, **13**, 2864–2869.
- 220 C. Zhu, J. Yuan, F. Cai, L. Meng, H. Zhang, H. Chen, J. Li, B. Qiu, H. Peng, S. Chen, Y. Hu, C. Yang, F. Gao, Y. Zou and Y. Li, *Energy Environ. Sci.*, 2020, **13**, 2459–2466.
- 221 R. Sorrentino, E. Kozma, S. Luzzati and R. Po, *Energy Environ. Sci.*, 2021, **14**, 180–223.
- 222 T. Liu, R. Ma, Z. Luo, Y. Guo, G. Zhang, Y. Xiao, T. Yang, Y. Chen, G. Li, Y. Yi, X. Lu, H. Yan and B. Tang, *Energy Environ. Sci.*, 2020, **13**, 2115–2123.
- 223 Z. Peng, K. Xian, J. Liu, Y. Zhang, X. Sun, W. Zhao, Y. Deng, X. Li, C. Yang, F. Bian, Y. Geng and L. Ye, *Adv. Mater.*, 2022, e2207884.